university of groningen

Master Thesis

Preparation of conductive coatings

Solution modification and CVD furnished coatings

Author:

Dāvis Kalniņš

Supervisors:

Ranjita Bose, PhD
prof. dr. Francesco Picchioni
prof. dr. Cor Koning

Daily supervisor:

Afshin Dianatdar

University of Groningen

Faculty of Science and Engineering

Chemical Engineering

August 26, 2019

Abstract

In this work, two distinct methods were applied to modify nanocellulose particles with a conductive polymer – polyaniline (PANI). The first technique was a solvent-based approach, via *in situ* polymerization, where these particles were dispersed in an aqueous medium using ultrasonication prior to the addition of the monomer aniline and then the drop-wise addition of the oxidant ammonium persulfate. The resulting composite materials had varying electrical conductivity values of 8.22×10^{-6} to 3.24×10^{-1} S/cm, dependent on the mass ratio between PANI and nanocellulose in the composite material. This material was successfully integrated in a polyurethane matrix, resulting in a conductive film exhibiting a conductivity of 2.14×10^{-4} S/cm.

The second method used in this project was chemical vapor deposition (CVD), in which nanocellulose particles were placed in a chamber under vacuum and exposed to vapors of the same monomer and the oxidant antimony pentachloride, resulting in very thin layers of PANI directly on the surface of the particles without the need of using additional solvents. Unfortunately, this approach did not yield a product with high enough conductivity, and further research has to be done to improve this technique.

Products obtained by both methods were analyzed using FTIR, TGA, XRD, CHNS elemental analysis and four-point probe conductivity measurement. Additionally, SEM and XPS was applied for the CVD furnished composites to prove the presence of any PANI content in the material.

Table of Contents

List of figures

List of tables

List of abbreviations

APS – ammonium peroxydisulfate

CP – conductive polymer

CNC – cellulose nanocrystal

CNF – cellulose nanofibrils

CSA – camphorsulfonic acid

CVD – chemical vapor deposition

DBSA – dodecylbenzenesulfonic acid

DMF – dimethylformamide

DMSO – dimethyl sulfoxide

EDS – energy-dispersive X-ray spectroscopy

FTIR-ATR – Fourier transform infrared spectroscopic method with attenuated total reflectance

FTSC – fluorescein-5-thiosemicarbazide

oCVD – oxidative chemical vapor deposition

PANI – polyaniline

PEDOT – poly(3,4-ethylenedioxythiophene)

PGMA – poly(glycidyl methacrylate)

pHEMA – poly(hydroxyethyl methacrylate)

P_m – partial pressure of a chemical compound at a specific temperature

P_{sat} – saturation pressure of a chemical compound at a specific temperature

PTFE – polytetrafluoroethylene

PTh – polythiophene

PU – polyurethane

S – saturation ratio

sccm – standard cubic centimeters per minute

SEM – scanning electron microscopy

TEMPO – 2,2,6,6-tetramethylpiperidine-N-oxyl

TGA – thermogravimetric analysis

THF –tetrahydrofuran

ICP – intrinsically conductive polymer

iCVD – initiated chemical vapor deposition

IR – infrared

VPP – vapor phase polymerization

XPS – X-ray photoelectron spectroscopy

XRD – X-ray powder diffraction

wt.% - weight percent

Introduction

In the current global society, there is an ever-increasing demand for new energy devices as a consequence of rapid technology development. This leads to a very significant demand for raw materials and inevitably also to serious environmental issues, such as pollution and the depletion of scarce natural elements like indium and gallium [1]. As a result, extensive research has been invested in the development of electrically conductive energy devices using carbon-based green materials. One of these green materials is nano-structured cellulose or nanocellulose in short. Produced by extracting from cellulosic materials at a relatively low cost, nanocellulose exhibits better mechanical strength, optical transparence and a smoother surfaces compared to its precursor [1]. Due to the electrically insulating nature of nanocellulose, it has to be combined with conductive materials to fabricate a composite that inherits the favorable properties of both components (Figure 1).

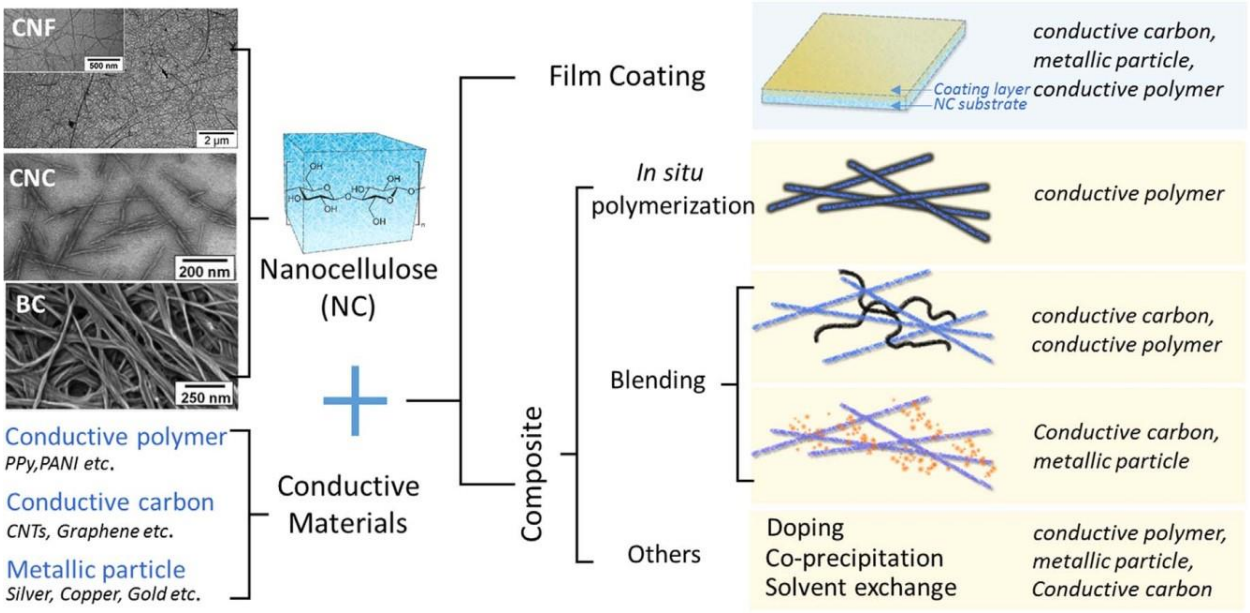

Figure 1. Nanocellulose based conductive composite material fabrication routes (source:[1]*)*

Conductive polymers have been widely used for this purpose. Generally solution methods are applied to synthesize the polymer and coat it on the chosen surface [2]. While convenient, this approach is not always feasible, especially when it comes to conductive polymers that tend to have very poor solubility and processability [3]. An alternative is to employ a non-solution-based technique – chemical vapor deposition (CVD). CVD is a process where the desired reaction is carried out in a reactor chamber commonly under vacuum, in which volatile precursors are injected. Depending on the necessary conditions,

parts of the chamber are either heated up or cooled down, and the chemicals in the gas phase react or break down to produce the desired product that accumulates on the surface of a chosen material [2], [4]. CVD has been extensively used in the semiconductor industry to produce integrated circuits [2], or in other areas where fabrication of high-performance thin films is needed, such as instrumentation, analytical flow path components, wear components, machine tools, and many other applications [4].

Within this group of materials, polyaniline (PANI) has been commonly recognized as one of the most important conductive polymers, due to its great electrical, optical, optoelectrical properties, environmental stability, and simple synthesis [5]. Conductive properties originate from its conjugated π-system, which unfortunately imparts it with high rigidity as well [6]. This may be mitigated by using a template material such as nanocellulose as a carrier for the polymer. The resulting conductive nano-particles can potentially be used as an electrically conductive filler for non-conductive polymers, which, due to the high aspect ratio of nanocellulose structures, might yield conductive polymer films at low nano-filler loadings [1].

In this present work two approaches to produce PANI coated nanocellulose have been carried out and compared: solution-based *in situ* polymerization and CVD coating. Both techniques have clear advantages and short-comings, which will be discussed further. This project explores the possibility of using DMSO as an alternative solvent to water for the solution-based approach, and if it has a positive impact on the conductivity of the end-product. Furthermore, it was investigated if it is possible to reliably coat nano-scale particles using the CVD method. Finally, these conductive rods made by covering high aspect ratio nanocellulose with PANI theoretically should impart the electrical conductivity property to a composite at low wt.% of loading, provided that the coverage is complete and the rods are not clustered, therefore the feasibility of using this product as a filler in polyurethane films to fabricate a composite with anti-static properties was inspected in this research.

Background information

In this chapter a brief introduction will be given to the two main building blocks of the conductive composite – nanocellulose and polyaniline, as well as a deeper look into research done about material modification with PANI coatings, and the potential applications of these composites as fillers. Finally, the CVD technique will be described in detail, including the recent advances in PANI thin film fabrication using this method.

Types of nanocellulose

Based on composition, properties and dimensions, three distinct categories of nanocellulose are known: cellulose nanocrystals (CNCs, known also as cellulose whiskers); cellulose nanofibrils (CNFs, known also as nanofibrillated cellulose (NFC), microfibrillated cellulose (MFC) or cellulose nanofibers); bacterial cellulose (BC, known also as microbial cellulose) [7]. Production of CNCs is generally done via acid hydrolysis, where cellulosic particles are dispersed in water, then exposed to an acid (sulfuric acid, for example) to dissolve the amorphous cellulose structures while leaving the crystalline regions intact [8]. Although this method can reliably produce CNCs with close to 90% purity, traces of sulfate groups can be found on the surface of these nanorods, due to the acid treatment [7]. The diameter and length of CNCs are 3 – 35 nm and 200 – 500 nm, respectively [7].

CNFs are fibrils typically a few micrometers in length and with a 5 – 50 nm diameter [7]. While CNCs have very high crystallinity, CNFs have a more even ratio between crystalline and amorphous domains [7]. Three techniques can be used to extract CNFs from cellulose fibers: chemical treatment (TEMPO-mediated oxidation or enzymatic hydrolysis, for example); mechanical treatment (milling, grinding, homogenization, for example); combination of both [7].

BC is produced via biosynthesis from bacteria, such as *Acetobacterxylinum*, and the cellulose is in its pure form, therefore further purification from contaminants like hemicellulose, lignin or pectin is not necessary. From this technique 20 – 100 nm long cellulose nanofibers can be acquired [7].

Intrinsically conductive polymers

Initially discovered in 1960, intrinsically conductive polymers (ICPs) amassed quite a large popularity in the material research sector due to their potential uses in fields such as electronics, electrochemical, electromagnetic, electromagnetic, thermoelectric, chemical, sensors, and membranes [3]. In reality there have been various obstacles that have made the usage of ICPs somewhat limited [3]. One of the main issues concerning the application of these polymers is their very poor solubility (and accordingly processability) in all known solvents, and simply the fact that the conductivity of ICPs is considerably lower than that of metal materials [3]. The problem with poor solubility, however, can be minimized in some cases, by using specific dopants or by chemically modifying the initial monomer [3]. A different approach is to blend the conductive polymer with another material that has superior processability and mechanical properties [3].

Figure 2 showcases a few known ICPs. ICPs have intrinsic electrical conductivity because the chemical structure contains a conjugated π-electron system [3]. These polymers generally have high electron affinity, low energy optical transition and ionization potential [3], [9]. The conductivity of ICPs

can change by undergoing oxidation-reduction reactions and based on the amount of dopant present in the structure [9], [10].

The conductivity, processability and stability of a number of conductive polymers can be seen in Table 1. Despite the impressive conductivity of polyacetylene, which is almost as high as copper, its processability and stability is quite mediocre compared to other ICPs [3]. A similar issue can be addressed to polyphenylene and its derivatives. While polyaniline, polythiophene and polypyrene are considerably less conductive, the other physical properties on the other hand are much better [3].

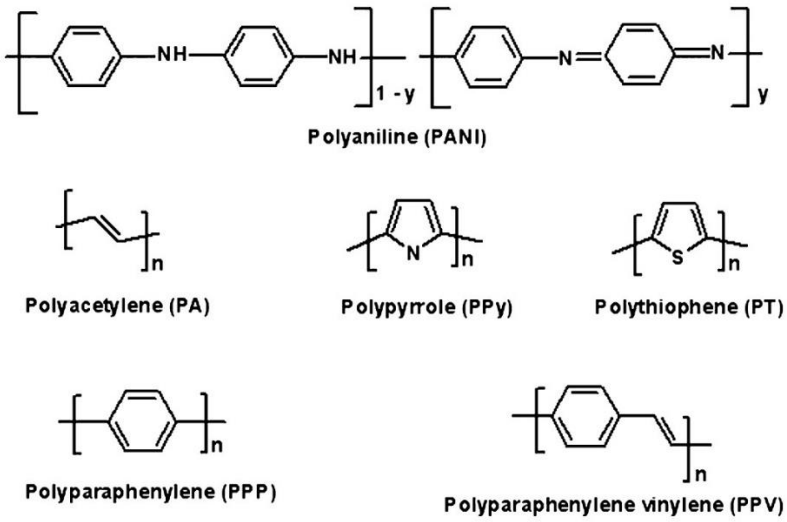

Figure 2. Chemical structures of some well-known ICPs (source: [3]*)*

Compared to the other conductive polymers in Table 1, PANI has better thermal stability and the monomer needed is significantly cheaper [3]. Also, the synthesis procedure of PANI is quite simple, while still leaving some room for adjustments to modify the properties of the end product, making it a very versatile polymer [11].

Table 1. A comparison in conductivity, processability and stability of a few conductive polymers (adapted from: [3]*)*

Polymer (doped form)	**Conductivity, S/cm**	**Processability**	**Stability**
Polyacetylene	1000 – 100000	Limited	Poor
Polyphenylene	1000	Limited	Poor
Poly(phenylene vinylene)	1000	Limited	Poor
Poly(phenylene sulphide)	100	Excellent	Poor
Polypyrroles	100	Good	Good
Polythiophenes	100	Excellent	Good
Polyaniline	10	Good	Good

Polyaniline

Initially PANI was known in 1835 as “aniline black”, which was a name given to any product stemming from the oxidation of aniline [12]. Even though this polymer has been known for over 180 years, thorough investigation in the potential of PANI only started in the 1980s after the discovery of conductive polymers. The aim of the research was mainly to study the chemical structure, conductivity mechanisms, polymerization mechanism of the polymer, and also to improve the processability via chemical and physical modification techniques [13].

Forms of polyaniline

The PANI structure (Figure 2) consists of two principal units:

- Unit containing two benzenoid groups (1-*y*);
- Unit containing one benzenoid and one quinoid group (*y*).

The redox state of PANI is dependent on the value of *y*, which theoretically can be in the range of 0 and 1 [14]. If *y* is equal to 1, PANI is in a fully oxidized form, pernigraniline, while *y* equal to 0 corresponds to the fully reduced state, leuceomeraldine. At an *y* value of 0.5 the polymer can have two different forms – emeraldine base, where PANI is completely undoped, and emeraldine salt, where it is doped (protonated) with an acid [14], [15]. Perngigraniline can be found in a salt form as well [14]. The different forms of PANI are depicted in Figure 3.

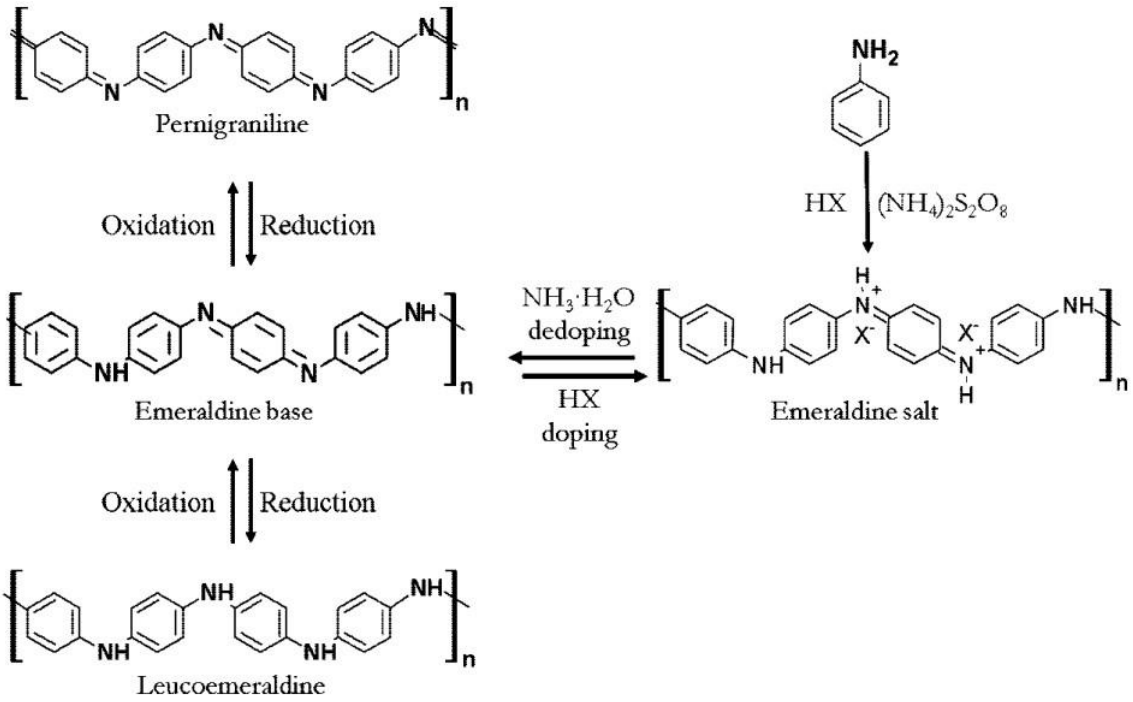

Figure 3. Synthesis diagram of polyaniline, showing the fully reduced and oxidized states (source: [13]*)*

The forms of PANI have different electron conductivities and colors, which are summarized in Table 2. Environmental stability can differ as well. Leucoemeraldine gradually oxidizes in air and has almost no electron conductivity, due to the fact that it only contains benzene rings and amino groups. The stability of pernigraniline is also relatively mediocre, because quinonediimine groups are unstable when exposed to nucleophiles. Even in the presence of water pernigraniline and its salts can decompose in air [14]. When emeraldine base is treated with an acid (either organic or inorganic), protons generally have a larger affinity towards the imino groups rather than the amino groups of the polymer, and as a result polycations are formed [14]. The cation radicals are delocalized over specific conjugation length, which in turn contributes towards the electron conductivity of PANI. This is also the reason why the conductivity of PANI is dependent on the degree of protonation. The conductivity increases by ten orders of magnitude, when the level of protonation changes from 0 % to 20 % [14]. This is a unique trait seen only in PANI. If the polymer chains are stacked together in one direction, cation delocalization may occur via an intermolecular mechanism, where Van der Waals forces between benzene and quinoid rings (π stacking) play a role [14]. PANI with such structured polymer chains can have surprisingly high conductivities: 1100 – 1200 S/cm [16].

Table 2. Different types of polyaniline and their physical properties (adapted from:[15]*).*

***y* value**	**Name**	**Color**	**Conductivity, S/cm**
0 (reduced form)	Polyleucoemeraldine base Polyprotoemeraldine base	Transparent	$< 10^{-5}$
0.5	Polyemeraldine base Polynigraniline base	Blue	
1 (oxidized form)	Polypernigraniline base	Purple	
0.5	Polyemeraldine salt	Green	≈ 15

Synthesis of polyaniline

The most common approach to synthesize PANI is via oxidative polymerization, where polymerization and doping occurs simultaneously [17]. This can be achieved either electrochemically or chemically. The electrochemical approach tends to give a purer product, but also generally has a lower yield compared to the chemical approach [14], [17].

Three reactants are necessary for the chemical approach: aniline, an oxidant, and an acidic medium. Figure 3 depicts the universal synthesis scheme of PANI. The synthesis mechanism can be separated into two stages [11]:

1. Slow athermic stage, where dependency on pH, reactant concentrations and temperature can be observed. Dissolved oxygen in the solution has no effect on the reaction as opposed to the

other oxidants in the mixture. This step conforms to the Arrhenius law in the temperature range from 0° to 50°C.

2. Fast exothermic stage, dependent on temperature, but not as much on the oxidant concentration [11].

Common acids used are hydrochloric acid (HCl) and sulfuric acid (H_2SO_4), although other types of acids can be used, such as camphorsulfonic acid (CSA), dodecylbenzenesulfonic acid (DBSA) and various polymeric acids, which consequently may improve the solubility, thermal stability of the product [15], [18]. The level of doping can be controlled by tuning the pH of the reaction mixture [13]. To prepare PANI in its electrically conductive form, being the emeraldine salt, the chemical reaction should occur in a very acidic medium, where the pH is between 0 and 3 [14], [17].

Based on recent literature the most commonly used oxidant for PANI synthesis is ammonium peroxydisulfate (APS) [17]–[24], but many other oxidants and combinations have been used with good results, such as the transition metal compounds of Fe(III), Mn(III), Mn(IV), Mn(VII), Cr(VI), Ce(IV), V(V) and Cu(II), noble metal compounds of Au(III), Pt(IV), Pd(II) and Ag(I), and chemicals such as KIO_3, H_2O_2 and benzoyl peroxide [25]. To avoid side reactions the reaction medium should be cooled down to 0 – 5 °C and the oxidant should be added dropwise. An aniline/oxidant molar ratio of ≤ 1.15 has shown to give a polymer of highest conductivity and yield, assuming the reaction is occurring in an acidic environment [17].

Surface modification of fibers and particles with PANI

PANI is a versatile polymer, and one potential application for this material is the coating of surfaces of different materials. This in turn modifies the end product, improving or giving new properties, the most relevant added property being electrical conductivity.

One of the simplest and most common methods to modify fibers and particles with PANI (and other conductive polymers) is *in situ* polymerization, where these substrate materials are in the presence of the necessary reactants of the polymer, synthesized in the same medium (Figure 4) [26].

When it comes to textile materials, forming emulsions using the polymer and a binder, and applying the paste directly to the material, is a suitable option as well. As an example, Teli *et al.* [27] had successfully coated a conductive polymer on polyester, wool and cotton fabrics, by making a coating paste from 5% PANI and a binder, then applying it directly to the textile and curing it at 150 °C for 1 min. This resulted in a substantial increase in bulk conductivity for cotton fabric from $\approx 10^{-9}$ to $\approx 10^{-4}$ S/cm and for polyester and wool from $\approx 10^{-10}$ to $\approx 10^{-5}$ S/cm [27].

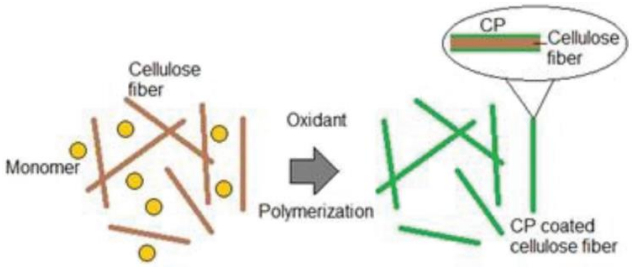

Figure 4. Cellulose fiber modification with a conductive polymer (CP) via in situ polymerization (source:[26]*)*

Large particle wood- and plant-based material modification

Hassel *et al.* [24] studied the morphology, electrical and mechanical performance of PANI-modified wood samples. Aniline monomer tends to penetrate wood veneer structures during polymerization, and PANI formation was mostly detected in cell walls and middle lamella [24]. A small decrease in maximum strength, ductility and storage modulus could be observed in the modified samples. The conductivity was found to be anisotropic and higher along the fiber direction (4×10^{-3} S/m) than across the fibers (4×10^{-4} S/m). An interesting side note is that lignin and PANI have a strong intermolecular interaction, due to the presence of aromatic structures and the hydrophobic characteristic of lignin [24], [26]. This resulted in an increase in glass transition temperature of the modified lignin [24].

To reduce the consumption of wood-based products, alternative sources of cellulose have been explored [26]. He *et al.* [28] worked with bamboo veneers to produce conductive bamboo/PANI composites. Depending on the level of doping using phosphoric acid, the conductivities of the materials were between 3×10^{-4} and 1×10^{-3} S/cm. Furthermore, the cellulose structure was still kept intact after the *in situ* polymerization, only with a slightly lower degree of crystallinity, as determined by X-ray analysis [28]. In a similar fashion Souza *et al.* [23] modified curauá fibers with PANI nanoparticles, achieving a 25 000 times increase in conductivity from 4×10^{-8} to 1.01×10^{-4} S/cm. Additionally, this material could have a potential use as a pressure sensor, as its conductivity changed up to 20 000% under applied pressure [23], [26]. In a different investigation mango fibers were utilized [29]. The composite material was not only 120 000 times more conductive than pure mango fiber, but also had innate magnetic properties as well [29]. Razak *et al.* [30] produced PANI/kenaf fiber composites. The kenaf fibers were treated with NaOH prior to the polymerization process to increase the -OH group amount on the surface and therefore the affinity for aniline monomers. The resulting material had only slightly reduced mechanical strength, but superior thermal stability and conductivity (5.25×10^{-3} S/cm) compared to pure kenaf fibers [30]. Bajgar *et al.* [31] modified cotton fabrics with PANI (and polypyrrole) to produce materials usable for monitoring plant neurobiology by using them in electrodes and collecting data from mechanical stimulation of the plant.

Nanocellulose modification

Several studies have explored the potential to combine PANI with bacterial cellulose (BC), due to their superior physical properties compared to conventional natural fibers [26]. Reports have shown that relatively high conductivity ($\approx 10^{-2}$ S/cm) values can be reached by modifying BC templates with PANI (doped with inorganic acids such as HCl), because the polymer can form a continuous "sheath" around BC fibers, due to the intermolecular attraction between amine groups of aniline and the hydroxyl groups of BC during the polymerization [26]. Marins *et al.* [32] conducted experiments using different amounts of DBSA in BC/PANI synthesis. It was found that the highest bulk conductivity (8.13×10^{-5} S/cm) can be achieved by having a DPSA/aniline ratio of 1.5. Excess amounts of DPSA facilitated the penetration of PANI into the bulk structure of BC fibers, as explained by the authors [32]. Despite that, having an even higher DBSA/aniline ratio promoted the accumulation of DBSA on the surface of BC, actually resulting in a lower conductivity for the end product. Müller *et al.* [33] reported to produce BC/PANI composite with a much higher conductivity (5×10^{-1} S/cm) using $FeCl_3$, where the molar ratio of oxidant/aniline was 2. Lee *et al.* [34] showed that impressive results can be achieved using p-toluene sulfonic acid as the dopant, having made a composite with conductivity of 1.3 S/cm.

Because large scale production and commercialization of BC is still considered problematic, other types of nanocellulose, CNCs and CNFs, could be considered a more attractive alternative for the fabrication of conductive cellulose-based nanocomposites [7]. Razalli *et al.* [19] produced CNC from Semantan bamboo, and coated it with HCl-doped PANI via *in situ* polymerization, and the electrochemical properties of these products were analyzed with cyclic voltammetry, by coating the composite on the electrode. It was reported that a higher current response was recognized in a PANI/CNC composite (84/16 ratio) compared to a pure PANI sample. This was explained by the higher level of protonation of PANI in the presence of CNC and the higher surface area of the nanocomposite, which might have positively impacted the electron transfer in the modified electrode [19]. Similarly, Casado *et al.* [35] observed an improvement in electrical conductivity for PANI/CNF composites (93/10 ratio) compared to pure PANI – 0.075 S/cm and 0.059 S/cm, respectively. This was due to the longer fibers present in the nanocomposite, which are more advantageous for electron mobility than the smaller particles and aggregates present in the pure sample, as explained by the authors. Yu *et al.* [6] tried to find the optimal experimental conditions to maximize the conductivity of the PANI/CNF composites. It was concluded that an aniline/CNF ratio of 2:1 and a 0.3 to 0.5 wt.% CNF concertation in the reaction mixture yielded the best results – 3.38 S/cm [6]. Silva *et al.* [36] produced PANI/CNF materials with varying monomer/oxidant and acid/monomer ratios, and molar ratios of 2 and 4, respectively, gave the best results ($\approx 10^{-1}$ S/cm). DBSA was used as the dopant, which had a secondary functionality as a surfactant and increased the stability of these composites in suspensions as well [36].

Inorganic material modification

Apart from the extensive research done on the surface modification of organic, wood- and plant-based materials, there have also been some reports on making composite materials with inorganic particles. PANI/ZnO nanocomposites in various ratios were successfully produced via the regular *in situ* polymerization method using CSA as the dopant [18]. While the resulting products had lower conductivities compared to pure ZnO nanorods and PANI, due to the adsorption of -NH groups of PANI on the surface of ZnO, these materials could have potential uses as antifouling and anticorrosive additives in marine paints [18]. In a different paper a PANI/diatomite composite was fabricated [5]. Diatomite is insulating by nature, and the addition of 8 wt.% of PANI increased its conductivity to 2.8×10^{-2} S/cm, and such a composite could have applications as a filler in conductive coatings and electromagnetic shielding materials [5].

PANI/cellulose material as a filler in polymer composites

Various papers have been published about the feasibility of using CP covered cellulosic materials as a conductive filler in polymer composites with the intention to add, for example, anti-static, electromagnetic or pressure-sensing properties to insulating polymer matrices [26].

PANI coated Curauá fibers were successfully blended with thermoplastic polyamide-6 using a twin-screw extruder. The resulting composites were reported to have a conductivity of around 10^{-7} S/cm [26]. The fibers facilitate better conductive pathways compared to pure PANI in a polymer matrix [26]. A different paper suggested the possibility to cure epoxy resins with PANI modified kenaf fibers, which can yield products with potential in anti-static applications [26]. For a material to be used for such a purpose it has to have a conductivity value in the range of $10^{-4} – 10^{-8}$ S/cm [37].

Merlini *et al.* [38] produced composites via compression molding using polyurethane (PU) derived from castor oil and PANI-coated coconut fibers. At 20 wt.% of conductive additive content in the PU matrix the resulting electrical conductivity was approximately 10^{-4} S/cm. The electrical resistivity of this material changed under compressive stress, therefore it might have a possible use in pressure-sensing applications [38]. Auad *et al.* [39] used PANI-modified CNF as a filler in PU memory foam. This was done by mixing a dispersion of PANI/CNF in dimethylformamide (DMF) with a DMF solution of PU in different weight percent ratios. It was reported that using the conductive filler resulted in a higher percolation threshold compared to non-modified CNF as filler due to particle agglomeration during PANI formation on the fibers. While electrically conductive PU composites were produced, filler contents higher than 4 wt.% negatively impacted the shape memory characteristic of the PU foam [39].

Electrically conducting composites consisting of polyvinyl alcohol and PANI/cellulose were fabricated by Anju and Narayanankutty [22] by adding the filler to the hot polymer solution in various amounts. In their research macro-, micro- and nanocellulose fibers were utilized and compared on the basis

of the resulting dielectric constant versus filler loading in the final composite materials. PANI-coated CNF fillers showed notably higher dielectric constant values across all concentrations, and a conductivity of 0.03 S/cm was achieved using this filler in the polymer matrix [22].

Chemical vapor deposition of polymer films

Polymer CVD has proven to be very effective in coating materials with thin layers of insoluble polymers, for example polytetrafluoroethylene (PTFE) and various electrically conductive polymers, such as polythiophene (PTh), poly(3,4-ethylenedioxythiophene) (PEDOT) and, more recently, polyaniline (PANI) [2], [40], [41]. It is a one-step technique to directly produce polymer coatings which are difficult to reprocess, for example polymers that only dissolve in very harsh, toxic solvents that might negatively impact the substrate, such as textiles, paper, plastic and membranes, or even negate undesired side reactions that could otherwise occur in solution phase, for instance in the case of poly(furfuryl methacrylate) [2].

Another significant advantage CVD has over other methods is the ability to control the thickness of the deposited layer, and achieve conformal coverage (*i.e.*, reliably coat the intricate contours) of micro- and nanostructures [2], [40], [42]–[44]. Almost any kind of material surface can be modified with CVD polymer films, and in some instances this approach is the only way to produce certain products [40].

The procedure of CVD is mainly controlled by the feed rates of the gases and by the pressure and temperature inside the reactor. Depending on the technique used, electric fields and photon fluxes may be implemented and adjusted as well [40]. Either homopolymer or copolymer films can be fabricated by feeding one or multiple monomers in the reactor. Apart from monomers, other species are introduced that are necessary for the polymerization reaction such as oxidants or initiator molecules, or inert gases that simply act as diluents [2], [40]. Oftentimes the reactants used are volatile liquids or solids instead of gases. In these situations the CVD chamber is operated at very low pressures and precursors are heated up to promote vapor generation [40].

To adjust the film growth rate, the concentration of the monomer absorbed on the surface, and the number-average molecular weight of the polymer, the saturation ratio, S, of the monomer has to be determined [40]. It is equal to the partial pressure of the monomer divided by the saturation pressure of the monomer at the operating temperature in the chamber – P_m/P_{sat}. At $S = 1$, condensation of gasses occurs in the reactor, which generally is unwanted as the residual liquid may create unreliable results in subsequent runs, if the CVD reactor is not adequately cleaned [40]. Due to this the CVD reactor is operated at much lower saturation ratios. This can be achieved by adjusting the maximum pressure and temperature in the chamber, as well as the flow rate of the feed.

Polymer CVD techniques

The two major CVD techniques used for polymer film synthesis are initiated CVD (iCVD) and oxidative CVD (oCVD). These methods are considered to be analogous to free-radical chain-growth polymerization and step-growth polymerization, respectively, which are well known synthesis mechanisms in solution chemistry [2]. Both iCVD and oCVD usually utilize commercially available precursors, and substrates typically do not need to be heated up to high temperatures. This combined with being completely solvent-free, makes these techniques attractive and convenient approaches to fabricate thin films and composite materials [2].

For the iCVD technique, a volatile thermal initiator is fed into the CVD chamber together with one or several types of monomers. Heated filament wires are present above the substrate that facilitate the thermal decomposition of the initiator to create active radicals. The substrate is typically cooled down to accelerate the monomer adsorption process on its surface, which then react with the present radicals, promoting polymer film growth on the material [2], [40]. Figure 5 depicts the reaction and mass transfer processes occurring in iCVD. Photo initiated CVD (piCVD) and initiated plasma enhanced CVD (iPECVD) are two variations of iCVD. Instead of just heat, in piCVD the decomposition of the initiator molecule is induced by UV light, while for iPECVD, low-plasma excitation triggers this effect [40]. Most of the iCVD films are electrical insulators and can be synthesized from various vinyl monomers, such as styrenes, acrylates, and methacrylates [40].

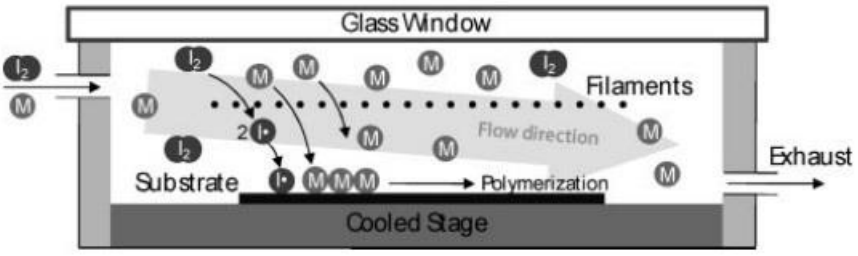

Figure 5. Schematic overview of the iCVD process (adapted from: [2]*)*

On the other hand, the oCVD technique can be applied to fabricate semiconductors and electrically conducting polymer films via step-growth polymerization directly on the surface of the substrate without the need of filament wires , UV-light, or plasma excitation [40], [45]. These conjugated polymers generally have a rigid backbone structure, making oCVD a better option compared to solvent-based methods, due to very poor solubility [2]. To successfully use this method, the main challenge is to find a suitable oxidant, as most have very poor volatility. Solid-state oxidants (e.g. $FeCl_3$, $CuCl_2$) have been previously used by putting them in a heated crucible inside the CVD chamber where they are sublimed by heating to ≈350 °C [40], [45]. A substrate is mounted above the crucible to be exposed to the vapors of the oxidant and the

monomer, which is introduced into the reactor from the side (Figure 6). Many conductive polymers have been synthesized with this method, including PEDOT that demonstrated very high conductivities (even above 2000 S/cm). This is comparable to products from alternative methods, such as solution casting and vapor phase polymerization (VPP) [45]. Liquid oxidants, such as bromine, vanadium oxytrichloride, antimony pentachloride have been used with good results as well [41], [46], [47]. In this case the oxidant can be delivered into the reactor in the same manner as the monomer, although through a separate line (as opposed to iCVD method where initiator and monomer mix together prior to entering the chamber), or otherwise the chemical reaction could start prematurely and the polymer would accumulate in the pipes.

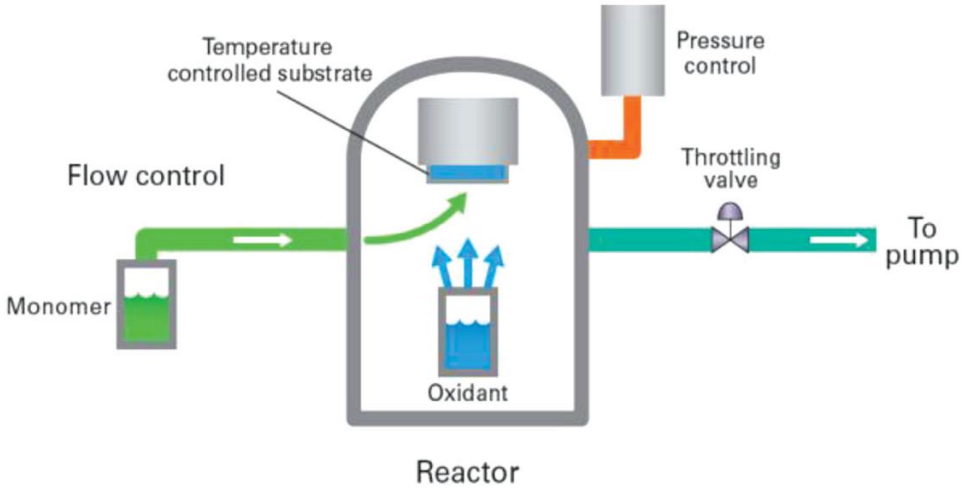

Figure 6. Schematic overview of oCVD process using a solid-state oxidant (adapted from: [45]*)*

Encapsulation of particles via CVD

As mentioned before, vapor-phase processing achieves high conformality of polymer films around complex micro- and nanostructured surfaces [40]. Extensive research has been done on the conformal coating of substrates containing nanopores or nanostructures (e.g. vertically aligned carbon nanotubes) [42], [48]–[52]. The CVD technique allows the polymer to penetrate and modify material surfaces that have complex contours with high precision. This can partially be accredited to the absence of the capillary effect and particle agglomeration, which is a considerable issue in solution-based alternatives [40].

In the case of aligned carbon nanotubes or pores, where each structure is individually separated, CVD is very effective. On the other hand, a much larger challenge arises if the objective is to coat bulk particles. Complete encapsulation of each individual structure can pose difficulties as there always is some contact between these particles, and some mixing followed by repeated coating may be necessary. Bose *et al.* [53] successfully encapsulated crop protection compound microparticles (nominal size of 3 µm) with different polymethacrylates via the iCVD method. For this procedure, 2 g of microparticles were evenly

scattered on a 75 mm diameter aluminum holder, and the process settings were adjusted to achieve an *S* of 0.7. Every 15 min the particles were taken out, thoroughly mixed, and then put back in the chamber to continue the deposition procedure, which lasted for 1 h in total. The coating thickness was estimated to be 330 – 594 nm, depending on the chosen CVD parameters [53]. Similarly, Baxamusa *et al.* [54] coated silica microspheres (50 – 100 µm) with hydrogel poly(hydroxyethyl methacrylate) (pHEMA) via piCVD, where the particles where manually agitated after every 100 nm of deposition until about 1 micron of the polymer was deposited.

Various experiments have been performed using modified CVD reactors with implemented rotary mechanisms to facilitate particle agitation. Lau and Gleason [55] successfully encapsulated carbon nanotubes (20 – 50 nm in diameters and 5 – 20 µm in length) and glass microspheres (average diameter of 28.5 µm) with poly(glycidyl methacrylate) (PGMA) using a rotary particle bed iCVD reactor. A schematic depiction of the setup can be seen in Figure 7. Conformality and stability of the coating was confirmed by the presence of a uniform fluorescent ring around the particles after being treated with an FTSC dye [40]. With a similar method, Parker *et al.* [56] achieved a conformal PGMA coating around pure and Al-coated NaCl particles. Compared to untreated NaCl, after the surface modification of pure and Al-coated particles, the dissolution rate reduced by one order of magnitude and almost two orders of magnitude, respectively.

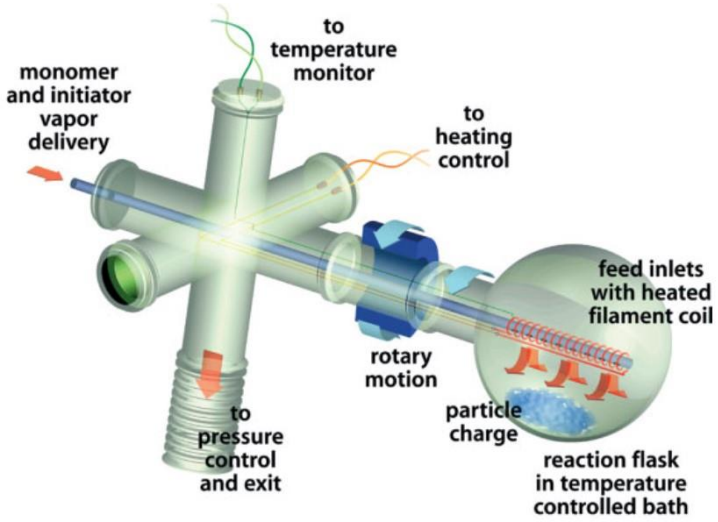

Figure 7. Rotary particle bed iCVD reactor (source: [55]*)*

Polyaniline synthesis via CVD

PANI synthesis using the CVD technique is a relatively new approach as most of the literature available has been published only in the last couple of years [41]–[44], [57]. Smolin et al. [41] studied the optimal oCVD processing conditions for PANI film fabrication on silicon wafers and quartz glass substrates using antimony pentachloride, $SbCl_5$, which functions both as an oxidant and a dopant. Nitrogen was used

as a diluent. Various experiments were carried out, changing specific parameters for the CVD process: reactor pressure from 35 mTorr to 700 mTorr; oxidant flow rate from 0.15 to 0.8 standard cubic centimeters per minute (sccm); and substrate temperature from 25 to 90 °C. Monomer and nitrogen flowrate were left unchanged – 1 sccm for both. The schematic process is depicted in Figure 8. Having a very low oxidant flow rate (0.15 sccm) promoted the formation of a less oxidized and a more oligomeric form of PANI. Similarly, having a substrate temperature of 25 °C yielded PANI in a more reduced state. On the other hand, changing the reactor pressure from 35 to 700 mTorr did not significantly impact the quality and the deposition kinetics of the polymer, therefore it can be assumed that PANI chemistry is not very pressure sensitive. Furthermore, some post-treatment was carried out involving washing the samples with THF with the intention to reduce the amount of impurities (excess oxidant and oligomers) on the film. While successful, this procedure significantly reduces the doping level of the polymer [41].

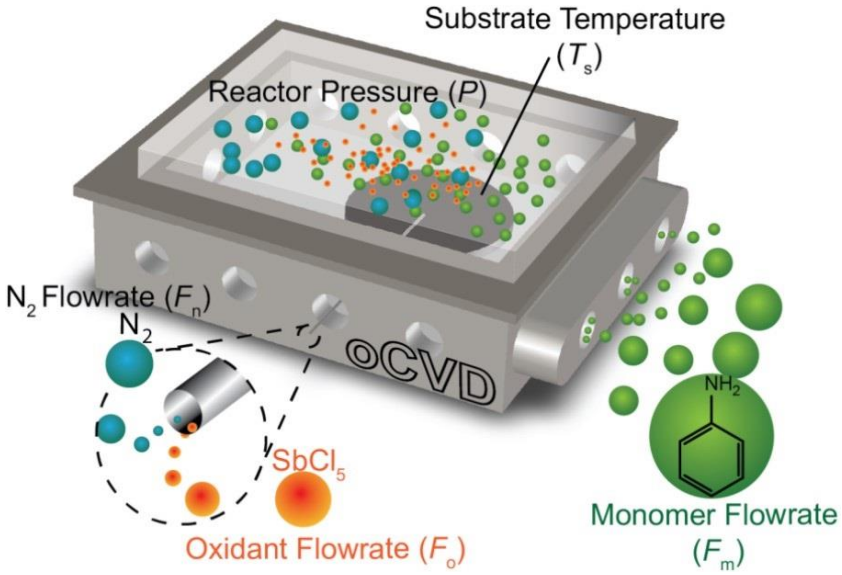

Figure 8. oCVD process for PANI synthesis displaying the essential parameters (adapted from: [41]*)*

Studies have shown a potential in using PANI as a conductive coating for porous carbon-based supercapacitor electrodes [42], [44]. Conformal coating was possible using oCVD with the aforementioned parameters. The resulting materials exhibited twice the gravimetric capacitance compared to unmodified carbon electrodes. Similarly, Li *et al.* [42] successfully coated an electrospun carbon nanofiber matrix, which then displayed high specific capacitance and good cyclic stability. Aniline, Nitrogen and $SbCl_5$ were fed into the reactor all at 1.5 sccm. An electrospun nanofiber mat was fastened in the chamber in an upright position to increase the contact area between the vapors and the fibers, and both the top and bottom part of the reactor were heated up to increase the temperature of the material to ≈60 °C [42].

Methodology

Two distinct methods were used to produce PANI coated nanocellulose particles, *viz.* solvent-based synthesis and CVD coating. These two techniques as well as the process of integrating the composite in a PU matrix will be described in detail in this chapter. Furthermore, the used materials and characterization methods will be mentioned here as well.

Materials

Aniline (99.5+ %, *Sigma-Aldrich*) was used without further purification, and either cellulose nanocrystals (CNC, diameter: 10-20 nm, length: 300-900 nm [58]) or cellulose nanofibers (CNF, diameter: 10-20 nm, length: 2-3 µm [59]) both bought from *Nanografi* were used for both techniques. For the solvent-based synthesis ammonium peroxydisulfate (APS, 98+ %, *Sigma-Aldrich*), (+)-10-camphorsulfonic acid (CSA, 98+ %, *TCI Chemicals*), hydrochloric acid (HCl, 37+ %, *Sigma-Aldrich*) and dimethyl sulfoxide (DMSO, 99.7+ %, *Sigma-Aldrich*) were used, all without purification. For the CVD method, as received antimony pentachloride ($SbCl_5$, 99 %, *Sigma-Aldrich*) was used as the oxidant instead. Silicon wafers (*UniversityWafers*, type: P) and microscope glass slides (76×26 mm, *Kittel-Glass*) served as substrates for pure PANI coatings. For modified PU films a dispersion of PU in water (40 wt.%, *NeoRez* R-1007) provided by *DSM* and sodium dodecyl sulfate (SDS, 97+ % *TCI Chemicals*) were used as received.

Solvent-based synthesis of PANI and PANI/CNC composites

PANI was synthesized via *in-situ* polymerization using aniline and APS in an acidic environment (pH ≈ 2). Either CSA or HCl in an approximately 1M concentration in distilled water was used. The monomer was dissolved in the acidic solution (1 – 2 wt.%) in a round bottom flask with a magnetic stirrer. In a separate vial APS was dissolved in distilled water (15 – 20 wt.%). Both solutions were cooled down in an ice bath for 1 hr prior to the start of the synthesis. Then the APS was added dropwise to the aniline solution in the span of 30 mins. The resulting aniline/APS molar ratio should be equal to 1. A temperature of 0 – 5 °C was maintained for approximately 5 hrs. Subsequently, the dark-green mixture was left stirring overnight. On the next day the precipitate was filtered using a Büchner funnel and washed several times with distilled water until the wash solution had become colorless. The solid product was then dried in a vacuum oven at 70 °C for 24 hrs.

Several products were synthesized using a mixture of water and DMSO in different volume ratios. This was done by separately dissolving aniline and APS in the aforementioned solution systems. The procedure was then carried out in the same manner as described above.

To produce PANI/CNC composites the CNC particles were dispersed in the acidic water solution (1 – 2 wt.%) using an ultrasonic bath (45 kHz, *VWR*, model USC300TH) for 1 hr, followed by the addition of aniline to the mixture and the regular experimental procedure. For comparison, some products were synthesized using the ultrasonic bath throughout the whole reaction process, instead of a regular magnetic stirrer. In this case the experiment was only carried out for 5 hrs before ending the reaction. Instead of using a Büchner funnel the PANI/CNC composite was isolated from the solution via centrifugation. This process was carried out at 4500 rpm for 20 min three times, mixing the solids with fresh distilled water in between the sessions. The solid product was dried in a vacuum oven at 70 °C for 24 hrs as mentioned before.

Substrate coating with PANI via the CVD method

The CVD procedure for depositing PANI films on different substrates was based on the previous research by Smolin *et al.* [41], although some adjustments had to be made to achieve satisfactory results for the custom-made CVD reactor used in this project. The setup of the reactor can be seen in Figure 9. Aniline and $SbCl_5$ were stored in vacuum sealed glass vials (length: 152 mm, diameter: 14.3 mm) and heated to 70 °C. Vapors were carried to the chamber through stainless steel tubes heated up to 110 °C to avoid condensation. A dry vacuum pump (*Edwards*, QDP80) was connected downstream of the CVD chamber to achieve a sufficiently low pressure. The reactor pressure was set to 700 mTorr, controlled by a downstream throttle valve connected to a pressure controller (*MKS Instruments*, type 651C) and a capacitance manometer (*MKS Instruments*, *Baratron* type 622C). Aniline, $SbCl_5$ and Nitrogen flowrates were set to 1.3 sccm, 2 sccm and 4 sccm, respectively. Flowrates were controlled using precision metering valves (*Svagelok*). Substrates were placed on a stage which was connected to a recirculating cooler (*Julabo* F250) to achieve a temperature of 40 °C. Glass slides, silicon wafers, CNC and CNF particles (≈1g evenly spread out in an aluminum tray) were used as substrates in the experiments. The CVD process was carried out for 10 minutes. In the case of CNCs and CNFs the coating was done twice. After the first round the particles were thoroughly mixed, before being put back in the chamber. As an additional precaution, a Teflon filter with a pore size of 0.2 μm was installed between the CVD chamber and the vacuum pump, when using the nanoparticles.

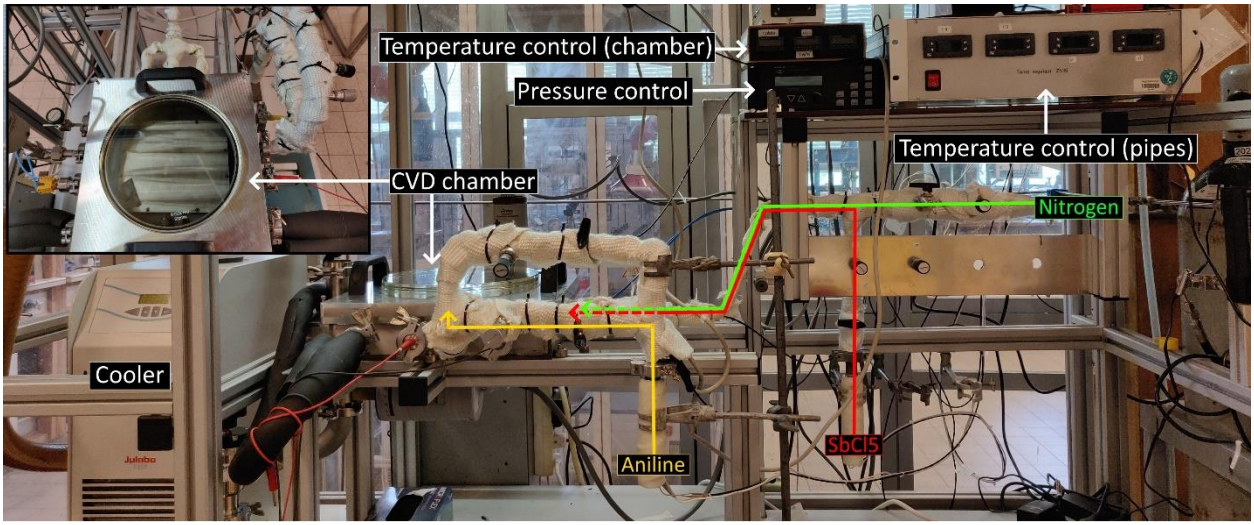

Figure 9. Side and top view of the CVD reactor, depicting the main components and chemicals involved in the CVD process.

Polyurethane modification with PANI/CNC particles

Some PANI/CNC samples from the solvent-based method were chosen to be mixed with aqueous PU dispersions to fabricate conductive films. After the synthesis and centrifugation, the PANI/CNC particles were put in an oven at 80 °C for 1.5 hrs, to get rid of excess water, but still maintaining a relatively high moisture content in the bulk material (10 – 20 wt.% water) to limit the irreversible agglomeration process of particles, which would frustrate the redispersion process. These particles were then re-dispersed in water by adding 2 wt.% SDS and using an ultrasonic bath for 3 hrs to produce aqueous dispersions of 2 wt.% PANI/CNC content. Both the PU and PANI/CNC dispersions were then mixed together in different ratios and poured in plastic Petri dishes, and left to dry in a fume hood overnight.

Characterization

Electrical conductivities of the materials were measured using a four-point probe system (*Ossila*, T2001A3). PANI and PANI/CNC powders were compressed into small pellets (thickness: 0.4 – 1 mm, diameter: 12.99 mm) and the conductivity was measured by placing the probes on one side of the material. IR spectra were measured using FTIR-ATR (*Shimadzu IRTacer-100*) in the range of 500 to 4000 cm^{-1}. The thickness of the deposited PANI on glass slides was determined via profilometry using a *Bruker DektakXT* stylus profiler with a 12.5 µm tip. Thermogravimetric analysis was done using a *PerkinElmer* TGA4000 by heating up the samples from 50 to 900 °C (20 °C/min) under nitrogen (20 ml/min). CHNS elemental analysis was carried out with a *Euro EA* elemental analyzer. XRD spectra were recorded using *Bruker D8 Advance* equipment in the range of 10° to 50° (0.018°/sec, X-ray generator: 40 kV, 40 mA). SEM analysis was done using a *Phillips* XL30 ESEM with an ≈8 mm working distance and an acceleration of 5 kV. XPS

analysis was performed at room temperature and in ultra-high vacuum conditions (base pressure < 10^{-2} mbar). All samples were deposited on gold surfaces (thin Au film grown on mica) by drop casting method. No further treatment was carried out prior to the XPS measurement.

Results and discussion

The experimental part of this project consists of six main objectives:

- Find the most optimal approach to synthesize PANI via the solvent-based method, considering the end goal – PANI/CNC composite fabrication in incorporation into PU films.
- When a successful PANI sample has been synthesized, introduce CNCs in the experimental procedure to produce PANI/CNC composite materials in various CNC and PANI ratios.
- Find optimal parameters to coat PANI on silicon wafers and glass slides using the CVD approach.
- Incorporate the use of CNCs to produce PANI/CNC composites via the CVD method.
- Compare the results of the solvent-based and the CVD techniques.
- Produce conductive blends of PANI/CNC and PU.

In the solvent-based approach initially HCl was used as the dopant for PANI synthesis, but because of the poor solubility, and conductivity alteration with moisture and temperature of the resulting HCl-doped emeraldine salts, other alternatives have been explored [15]. Due to this, CSA was chosen as a substitute for several reasons. Firstly, it has been previously reported that CSA-doped PANI exhibits improved solubility in some organic solvents such as DMSO and *m*-cresol improving its processability [15], [60], [61]. Furthermore, CSA-doped PANI has been stated to have higher conductivity values compared to the HCl-doped polymer [3], [60]. Finally, to our knowledge, there have not been any reports on producing PANI/CNC composite materials using CSA as the sole doping agent, making it a novel approach.

It should be noted that CSA-doped PANI generally has been produced via secondary doping, meaning that the PANI salt is initially synthesized using HCl, then de-doped to produce a PANI base, and finally doped again using a solution of the desired acid [60]–[62]. This is not a feasible option in the context of this project, as the end goal is to be able to reliably produce PANI/CNC composite materials through the means of one-step *in-situ* polymerization with CNC particles present in the reaction mixture, and the consecutive de-doping and re-doping processes might disrupt the composite structure.

It has been previously assumed that polyaniline products with higher molecular weights exhibit better electrical charge transport [63]. A hypothesis was made that replacing water in the reaction with another solvent in which the product might have better solubility would slow down the precipitation process, keep the growing polymer chains longer solubilized and extend the chain growth period of the polymer, resulting in a higher molecular weight product. To find out if the chosen solvent can affect the

conductivity of the end-product, several experiments were carried out using different volume ratios of H_2O and DMSO in the reaction system. The results can be seen in Table 3. Note that using pure DMSO is not possible because the freezing point of this solvent is around 18 °C while the experiment is carried out at 0 to 5 °C and some water has to be present in the reaction mixture [64].

Table 3. Reaction solvents (DMSO and H_2O) effect on the conductivity values of synthesized PANI products (doping agent: CSA).

No.	**H_2O/DMSO**	**CNC/Aniline**	**Conductivity, S/cm**	**Other notes and conditions**
D1	10/90	-	3.63×10^{-2}	
D2	25/75	-	6.94×10^{-5}	
D3	50/50	-	2.07×10^{-2}	
D4	50/50	60/40	3.24×10^{-1}	CNC in ultrasonic bath for 1 hr prior to reaction
D5	75/25	-	2.10×10^{-2}	
D6	Only H_2O	-	9.65×10^{-1}	

PANI synthesized in water showed the highest electrical conductivity, and there does not seem to be a clear correlation between solvent volume ratio and conductivity. That being said, the addition of DMSO did affect the time when color change started happening in the reaction mixture (from transparent to dark blue/green), which is tied to the precipitation kinetics of the reaction. For example, the color change in experiments D1 and D2 started only after 3 – 4 hrs, while for D5 and D6 after 20 min. Interestingly, experiment D4 resulted in a product with a higher conductivity value compared to other batches where DMSO was used. This could allude to the possibility that having a high aspect ratio material as a template for PANI might positively impact the mobility of electrons in the bulk material, although compared to D6 the conductivity was still lower.

As a side note, previously synthesized HCl-doped PANI had only a slightly lower conductivity value (8.75×10^{-1} S/cm) compared to CSA-doped PANI (experiment D6). However, these results are still considerably lower than the expected value based on previous literature – ≈15 S/cm [15]. Additionally, changing the doping agent did not seem to improve the solubility of the end product in organic solvents, although no additional analysis was done to prove or disprove this as it was not the main focus of the project.

Table 4. Effect of CNC and Aniline ratio on conductivity in PANI/CNC composites (doping agent: CSA). Note: ultrasonic bath was used for 1 hr on the CNC dispersion prior to the start of the reaction unless otherwise stated.

No.	CNC/Aniline	H_2O/DMSO	Conductivity, S/cm	Other notes and conditions
C1	Only aniline	-	9.65×10^{-1}	No ultrasonic bath
C2	16/84	-	3.06×10^{-2}	
C3	50/50	-	3.57×10^{-2}	Ultrasonic bath for the whole experiment
C4	50/50	-	6.78×10^{-2}	No ultrasonic bath
C5-1	60/40	-	**2.82**	
C5-2	60/40	-	**6.23×10^{-2}**	
D4	60/40	50/50	3.24×10^{-1}	
C6	90/10	-	8.22×10^{-6}	

Based on the previous results it was decided to pursue the use of H_2O as the sole solvent for the PANI/CNC synthesis. Several experiments were carried out using different mass ratios of CNC and aniline in the reaction mixture to see the effect on electrical conductivity (Table 4). An outlier in this list is C5-1, which had an unexpectedly high conductivity value – 1 to 2 orders of magnitude higher than other results. For this reason, this experiment was repeated (C5-2) to see if this result can be reproduced, which was not the case, as the new value was more in line with other results. Apart from C5-1, an increase of CNC content from 16 to 60 did not significantly impact the conductivity of the end product. It was also investigated if the use of an ultrasonic bath for the whole duration of the experiment might affect the outcome (C3). Compared to experiment C4 where no ultrasonic bath was used at all, the difference is negligible, although it is assumed that agitation of CNC particles leads to better dispersions and therefore to more homogenous PANI/CNC products.

To summarize, Figure 10 depicts the dependence of electrical conductivity of synthesized products on the H_2O/DMSO volume ratio and the CNC/Aniline mass ratio. As stated before, the addition of DMSO during the synthesis procedure did not improve the conductivity of PANI products, but had a clear opposite effect when compared to the result of a conventionally produced polymer in an aqueous medium. A similar conclusion can be drawn from the second group of experiments where conductivity is compared to the added CNC. In most cases the addition of either DMSO or CNC resulted in a conductivity value at least one order of magnitude lower than that of pristine PANI produced in pure water. An outlier is experiment D4, which was synthesized in 50/50 (H_2O/DMSO) mixture and having a CNC/Aniline ratio of 60/40. It is not clear why it has a considerably higher conductivity value than other experiments (apart from pure PANI) and further research should be carried out to see if it is possible to reproduce this result.

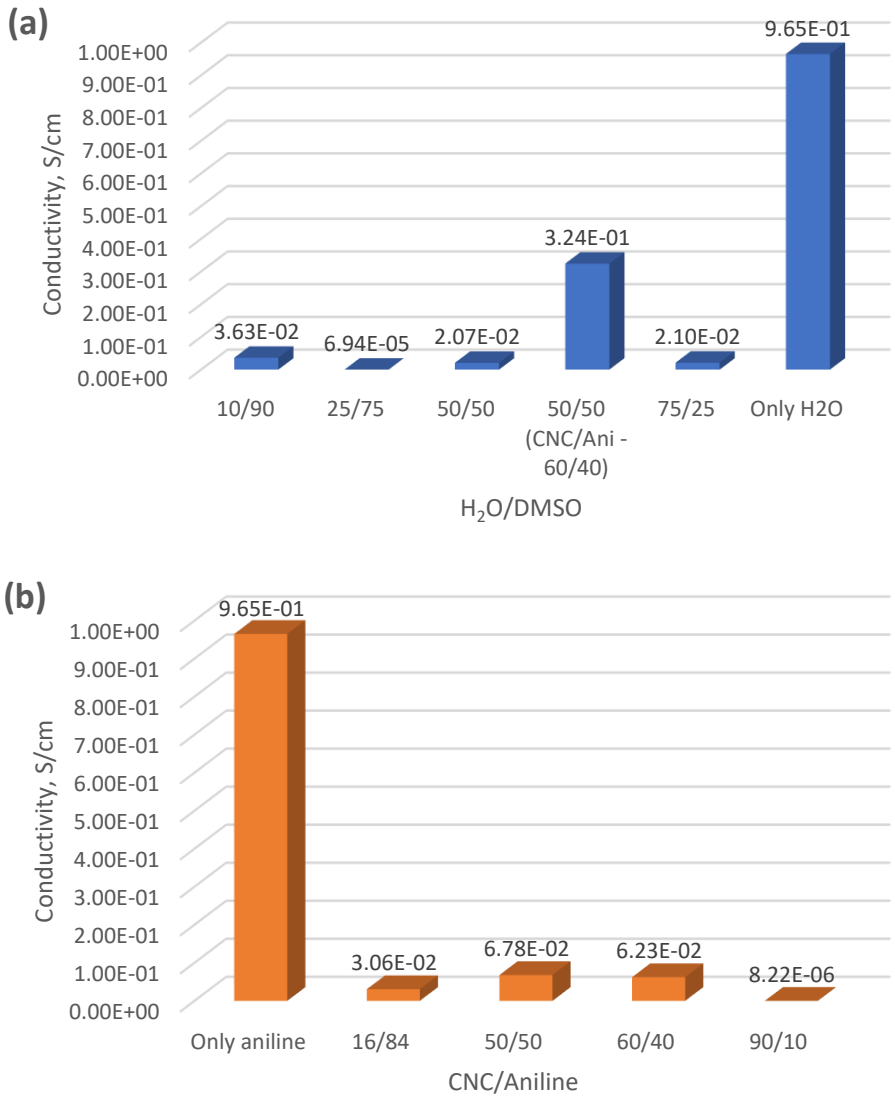

Figure 10. Conductivity dependency on (a) H_2O/DMSO ratio and (b) CNC/Aniline ratio.

While PANI synthesis through CVD is not a completely novel approach, it still posed a challenge as some adjustments had to be made to accommodate the design of the custom-made CVD reactor used in this project. Previous findings of Smolin *et al.* [41] served as the initial template for the experimental work. That being said, using the same parameters (gas flow rates, in particular) resulted in the accumulation of PANI around and in the oxidant/nitrogen CVD chamber inlets. This was especially concerning, as it could lead to clogging in the pipes, and make cleaning nearly impossible, due to the very poor solubility of the polymer. To mitigate this, significantly higher flow rates of $SbCl_5$ and nitrogen were used. This resulted in a saturation ratio, *S*, of around 0.12 and 0.21 for aniline and $SbCl_5$ vapors, respectively.

A successful coating of PANI on a glass slide sample can be seen in Figure 11. Picture (a) depicts a comparison of an untreated glass slide and a treated one. Based on profilometry results the thickness of

these films were in the range of 1210 – 1714 ± 20 nm, and conductivity values of 0.0329 – 0.0551 S/cm were measured by the four-point probe, which is around 18-29 times lower than the conductivity of pure PANI from the solvent-based approach. A clear color change could be observed after taking out the sample from the CVD chamber, seen in picture (b). The initially yellow/orange coating gradually changed to a green color. It is not known why exactly the PANI product gains its characteristic emeraldine salt color only after the end of the experiment. The reaction between the monomer and $SbCl_5$ might not have fully completed after the initial deposition, as the initial yellow/orange tint had a closer resemblance to the colors of the used precursors. It should be noted that these coatings are not completely homogeneous, based on the clear color intensity differences between separate regions on the coated samples. This is due to the relatively high flow rates used in the experiments, which resulted in a more turbulent vapor flow rather than laminar. As a consequence, the coating process is not as predictable, and batch-to-batch variations in film thickness were observed. Nevertheless, the results were deemed acceptable enough to progress towards the use of CNC and CNF particles as templates for the PANI deposition.

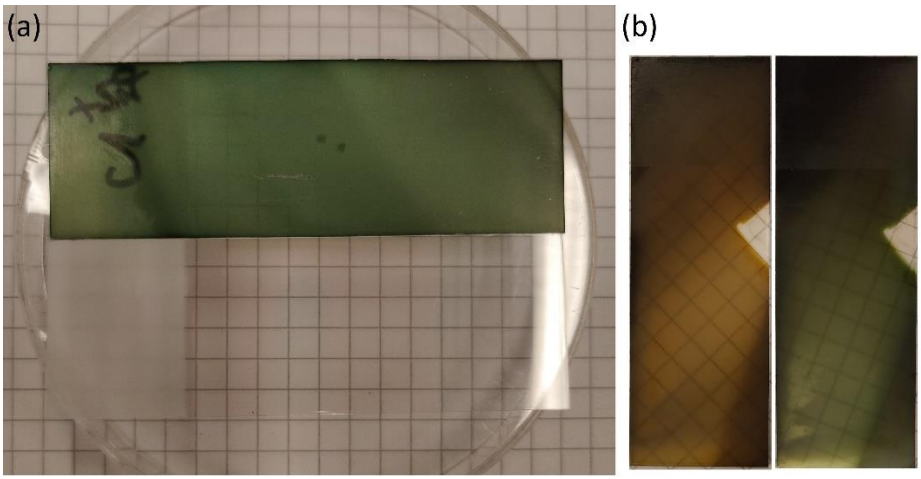

Figure 11. (a) Glass slide coated with PANI via the CVD method (top) and an uncoated glass slide for comparison (bottom). (b) Coated glass slide just after taking out of the CVD chamber (left) and the same sample after approx. 30 min (right).

For the modification of nanocellulose particles via CVD the same parameters were used as for the aforementioned PANI film fabrication. After the two consecutive CVD cycles a clear color change from light beige to greyish-green could be observed (Figure 12). Similarly, to the PANI/CNC composite from the solvent-based approach, the product was compressed into pellets to measure the bulk conductivity of the material. Unfortunately, the product did not have sufficient conductivity to be measured by the four-point probe. The amount of PANI present was too small to significantly affect the physical properties of the material. Due to this, this product was not further used as a filler for PU films.

Figure 12. From left to right: untreated CNF, CNC samples, and PANI/CNF, PANI/CNC products acquired from CVD.

FTIR analysis

FTIR spectra for pure PANI products from the solvent-based (CSA-doped) and the CVD technique can be seen in Figure 13. It is observed that doped PANI products tend to have relatively high overall absorbance in the 600-1600 cm^{-1} range and distinguishing individual peaks can be challenging. Nevertheless, several characteristic PANI absorption bands can be identified for the solvent-based sample, namely the C=C stretching vibration of the quinone ring and the benzene ring at 1552 and 1474 cm^{-1}, respectively, the C-N stretching vibration of secondary amine at 1287 cm^{-1} and the $C\text{-}N^{+\bullet}$ stretching vibration in the polaron structure at 1234 cm^{-1} [6], [36], [65]. The broad band around 1000 cm^{-1} can be attributed to $\text{-}NH^{+}\text{=}$ stretching, in-plane C-H vibrations of the PANI benzenoid ring or to S=O vibration from CSA [18], [41], [66]. C-H out-of-plane bending vibrations and/or C-C, C-H vibrations of the aromatic ring can be assigned to the peaks at 873 cm^{-1} and 762 cm^{-1} [18], [36], [41]. PANI produced from the CVD method (deposited on a silicon wafer) has a relatively similar spectrum, exhibiting peaks in the same range as its conventionally synthesized counterpart.

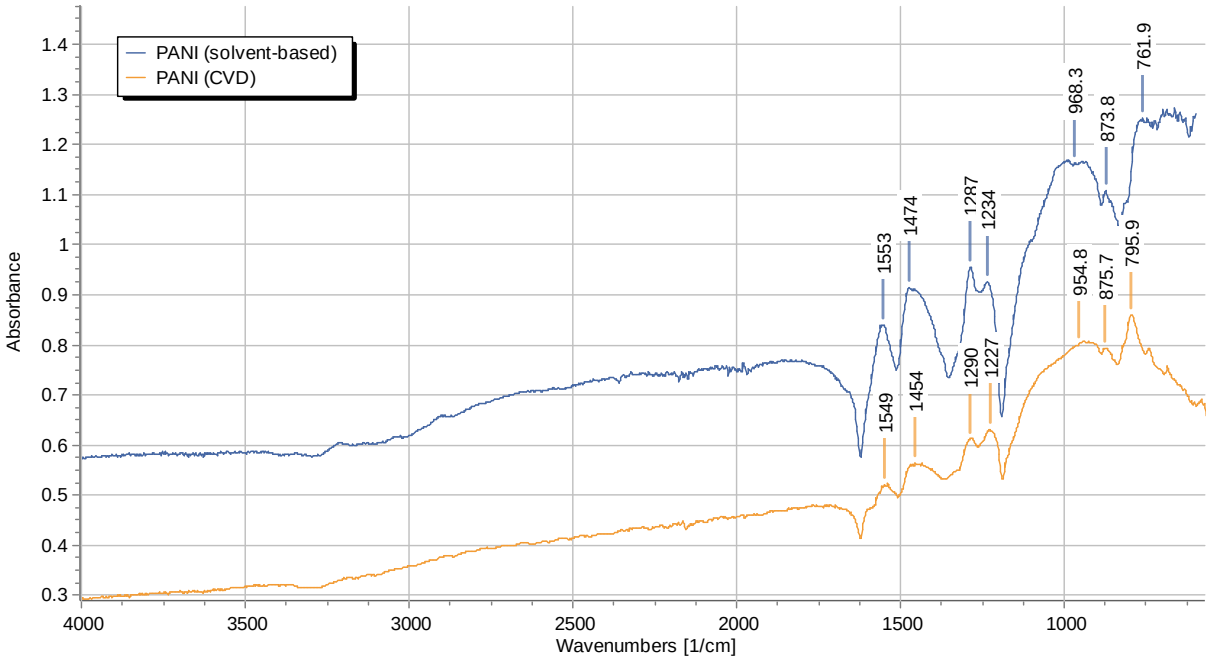

Figure 13. FTIR spectra of PANI synthesized via the two distinct approaches.

Figure 14 depicts three different spectra: untreated nanocellulose and two different PANI/CNC composite materials with an aniline/CNC mass ratio of 1:1 and 1:9. Characteristic absorption bands of nanocellulose can be identified in the spectrum of the untreated sample, such as the O-H stretching due to H-bonds at 3356 cm^{-1}, the C-H stretching vibration in the pyranoid ring at 2898 cm^{-1}, the O-H deformation due to H_2O at 1599 cm^{-1}, the -OCH in-plane bending at 1427 cm^{-1}, the C-H deformation at 1351 cm^{-1}, the C-O-C asymmetric stretching vibration at 1153 cm^{-1}, the glucose ring stretching vibration at 1111 cm^{-1} and the C-O stretching vibration at 1052 cm^{-1} [19], [36]. For the 1:1 mass ratio sample only certain PANI specific peaks can be distinguished (1551, 1443, 1284 and 1229 cm^{-1}), obscuring the CNC peaks, which could be caused by an overall CNC surface coverage with PANI in the examined region. In the 1:9 sample the concentration of PANI is significantly lower, resulting in a FTIR spectrum where several characteristic absorption peaks from both components can be seen. There is a clear overlapping of these absorption bands, and some intensity differences and minimal shifts in the peak signal values can be observed, when comparing these spectra.

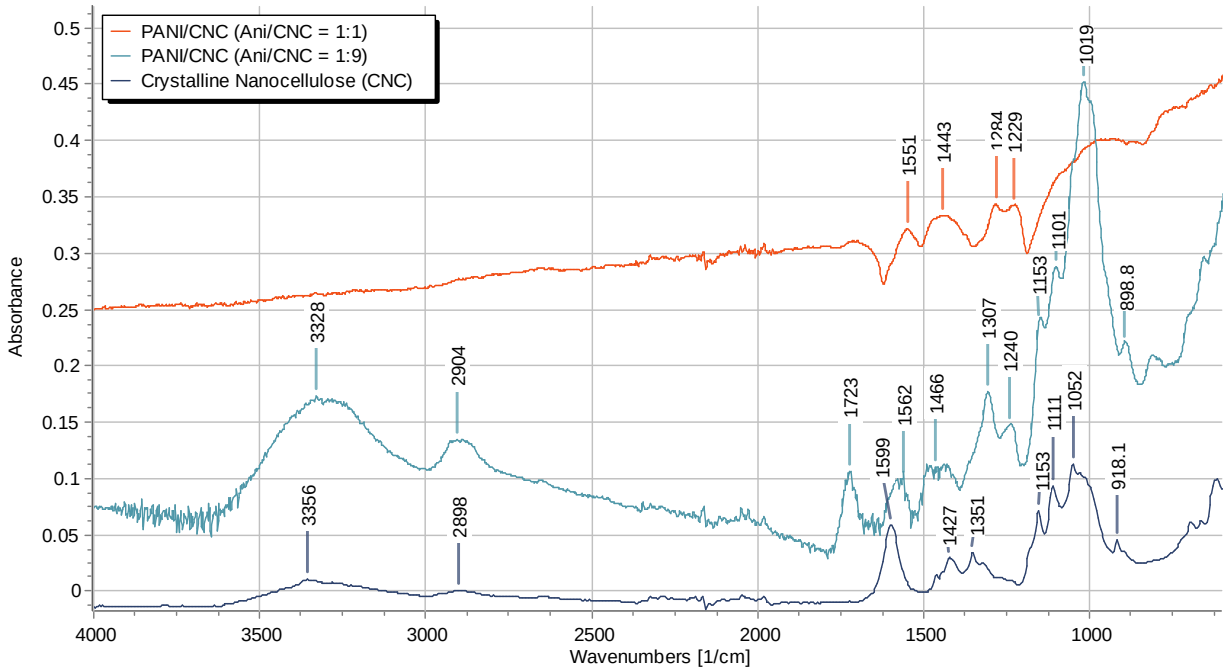

Figure 14. FTIR spectra of untreated nanocellulose (CNC) and two PANI/CNC composites synthesized by solution polymerization using Aniline/CNC mass ratios of 1:1 and 1:9.

In Figure 15 spectra of nanocomposite samples from the CVD method are compared to untreated samples. In all cases only the relevant peaks of nanocellulose can be identified but not those of PANI. It can be concluded that the PANI concentration in these products are significantly lower than 12 wt.%, when compared to the FTIR spectrum of PANI/CNC (Ani/CNC = 1:9) sample from Figure 14 where the estimated PANI content is approximately 12 wt.%, and therefore other quantitative and qualitative analysis methods have to be applied to confirm the presence of this polymer in the CVD products.

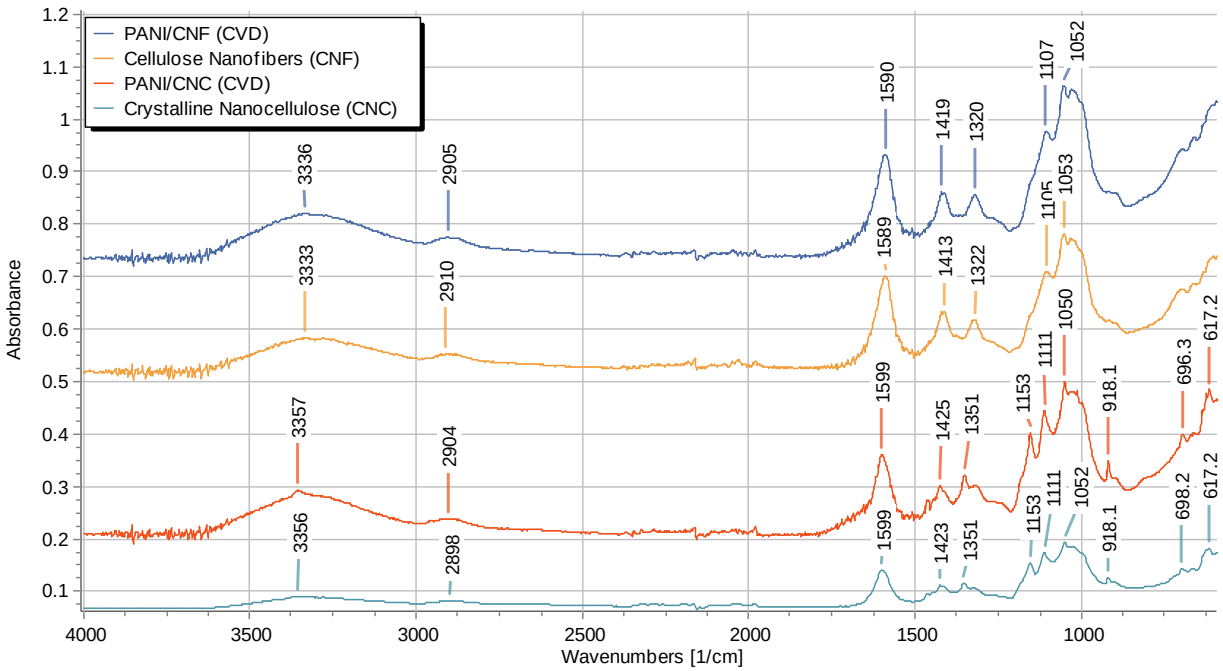

Figure 15. FTIR spectra of untreated CNC and CNF, and PANI/CNC, PANI/CNF produced from CVD.

Thermogravimetric analysis

TGA was performed for several samples to look at the thermal stability of the nanocellulose/PANI nanocomposites. Figure 16 depicts TGA curves for pure PANI (CSA-doped and HCl-doped), pure CNC and PANI/CNC composites fabricated by the solution polymerization method with varying aniline and CNC mass ratios. CNC had a very sharp drop in mass percentage to 52 % starting from around 280 °C to 350 °C, while for pure PANI mass loss happened in a more gradual fashion. It should be noted that CSA-doped PANI started undergo considerable mass loss at around the 200 °C mark, due to CSA decomposing at this temperature [67], while the HCl-doped sample started losing mass even at 50 °C, making it less thermally stable. Based on the PANI/CNC curves, it can be concluded that increasing the CNC content in the product results in greater mass loss, which can be seen in the 350 – 550 °C range. A similar trend for TGA data has been observed previously, mixing HCl-doped PANI with nanocellulose instead [19], [33], [68]. Above 700 °C the data is difficult to interpret, which could be due to possible char forming or crosslinking happening during analysis in this temperature range, although this is still uncertain.

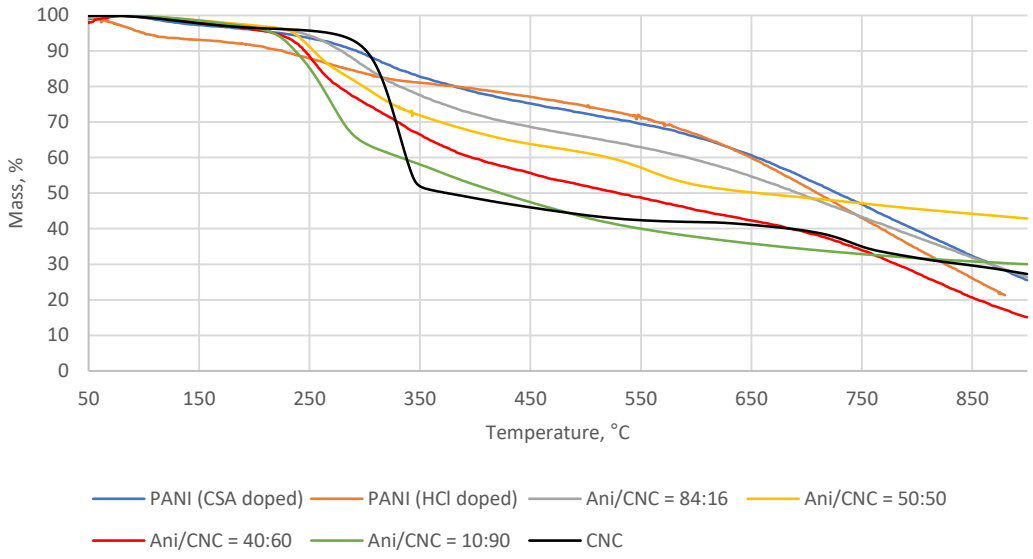

Figure 16. Effect of aniline/CNC ratio on the thermal stability of PANI/CNC composites prepared via the solvent-based method.

Figure 17 shows TGA curves of CNC, CNF and PANI/CNC, PANI/CNF produced via the CVD method. These curves are relatively similar to each other, depicting a sharp decline in mass percentages in the range of 280 to 370 °C. Just like FTIR this analysis method does not give conclusive data of the PANI content in these samples.

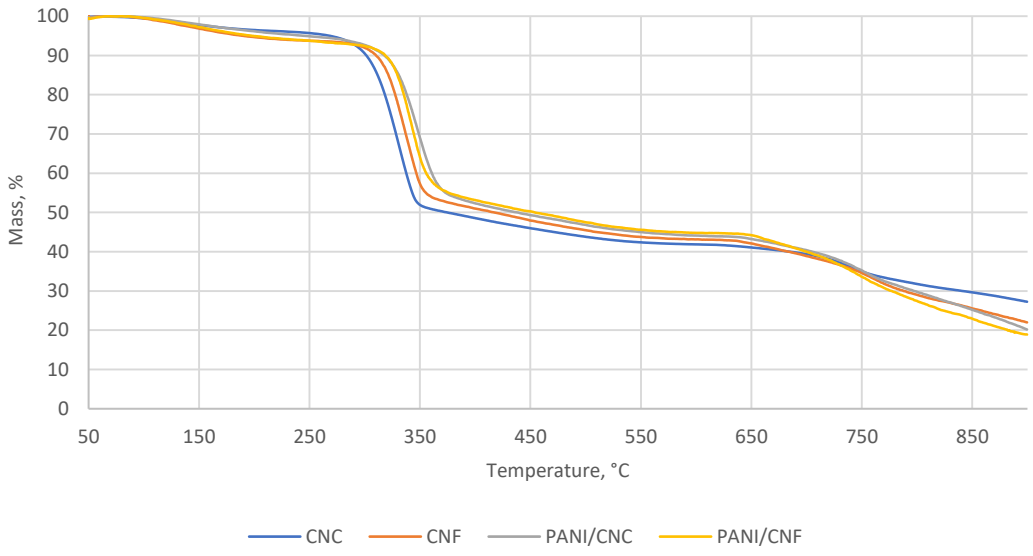

Figure 17. CVD produced PANI/CNC and PANI/CNF thermal stability compared to untreated nanocellulose.

XRD analysis

XRD analysis is a widely used tool to evaluate the crystallinity of various samples. These XRD patterns can also serve as a "fingerprint" for specific materials and therefore, for example, can give an indication of the presence of specific components in a composite material. Figure 18 shows XRD patterns of pure PANI, CNC and a PANI/CNC composite prepared by the solvent-based method. Three characteristic PANI peaks at around 2θ = 14°, 20° and 25° can be identified in the diffractogram [69]. Peaks at 2θ = 20° and 25° correspond to the (020) and (200) crystal planes, respectively, which indicate that the polymer is in the emeraldine salt form [19]. Distinctive peaks at 2θ = 14°, 22° and 35° can be seen in the CNC diffractogram, associated with the (110), (200), and (004) planes, respectively, characteristic for cellulose type I [19]. Other peaks were not identified, but indicate the high crystallinity of this material. The XRD pattern of the PANI/CNC composite material retained the characteristic peaks of both components – at 2θ = 14°, 20°, 22°, 25°, and 35°.

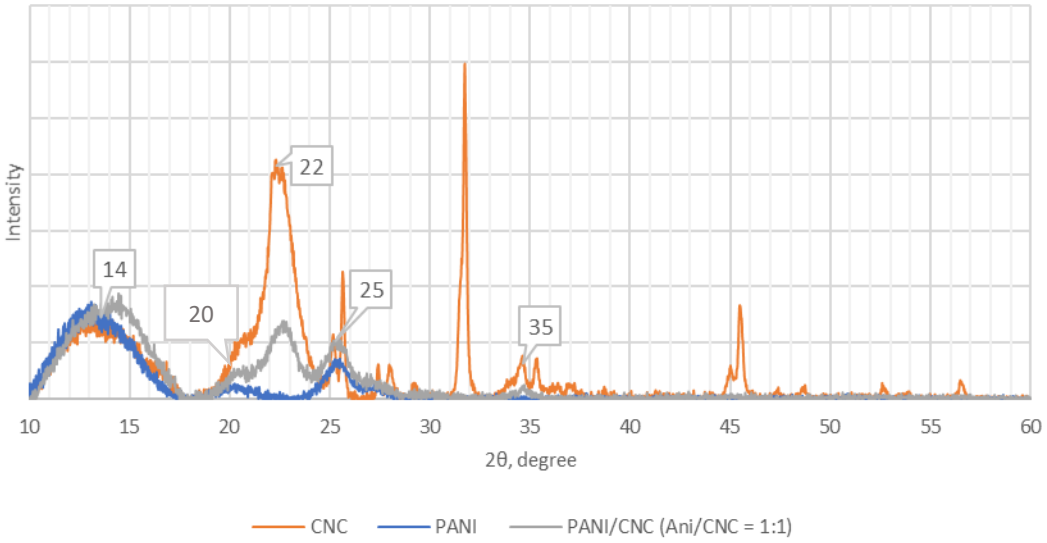

Figure 18. XRD diffractogram of untreated CNC, PANI, and PANI/CNC composite (aniline/CNC ratio – 1:1) prepared by the solvent-based method.

As expected, based on previous data from FTIR and TGA, neither could XRD analysis confirm the presence of PANI in the composites produced by the CVD technique. The X-ray diffractogram of the CVD sample (Figure 19) closely resembled the pattern of untreated CNC, exhibiting peaks in the same range. This is obviously caused by the extremely low quantities of PANI deposited on the CNCs.

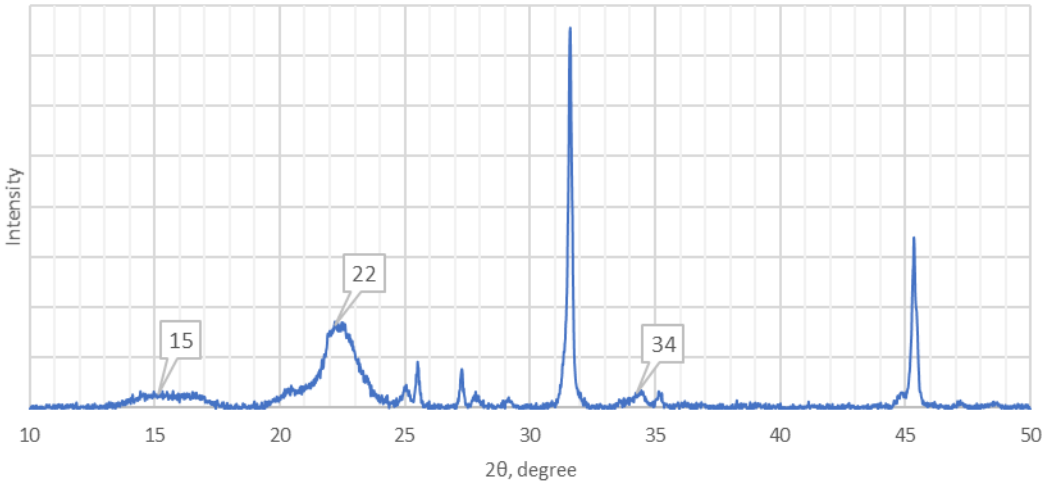

Figure 19. XRD diffractogram of a PANI/CNC sample fabricated via CVD.

CHNS elemental analysis

Elemental analysis was carried out for a few samples to get a better understanding of the doping level of the solvent-based products and the overall PANI content in the CVD furnished composites. Weight percentages of elements N, C, N and S in the synthesized products as well as in the untreated nanocellulose samples are summarized in Table 5.

Table 5. CHNS elemental analysis results of untreated CNC, CNF, PANI, and PANI/CNC, PANI/CNF composites. Note: The C and H content of samples No. 6 and 7 were not measured.

No.	Name	Dopant	N [%]	C [%]	H [%]	S [%]
1	CNC	-	0.00	34.49	4.80	1.75
2	CNF	-	0.00	33.67	4.81	1.36
3	PANI/CNC (via CVD)	$SbCl_5$	0.02	33.82	4.76	1.20
4	PANI/CNF (via CVD)	$SbCl_5$	0.03	33.28	4.78	1.06
5	PANI/CNC (CNC/Ani = 90:10)	CSA	1.01	42.94	6.07	2.24
6	PANI/CNC (CNC/Ani = 50:50)	CSA	6.76	-	-	4.49
7	PANI	CSA	11.03	-	-	5.59

It is assumed that to some extent the conductivity of PANI is dependent on the acid doping level of the polymer [14]. Due to CSA being a sulfonic acid, the S content in these samples can be directly related to the doping intensity, if the structure of the polymer is known. It was assumed that the synthesized PANI products would resemble the proposed structures illustrated in Figure 20(a), where the calculated N, C, H, S content (weight based) for a CSA-doped polymer is 6.78 %, 63.92 %, 6.05%, and 7.75 %, respectively. It should be noted that some S content was detected in untreated nanocellulose as well, which has to be

taken into account when estimating the CSA content in PANI/CNC products. Considering the theoretical structure of PANI and the data in Table 5, the doping level (CSA) in samples No. 5, 6, and 7 were 74.42 %, 90.38 %, and 72.08 %, respectively, based on the theoretical maximum and the polymer content in the composites.

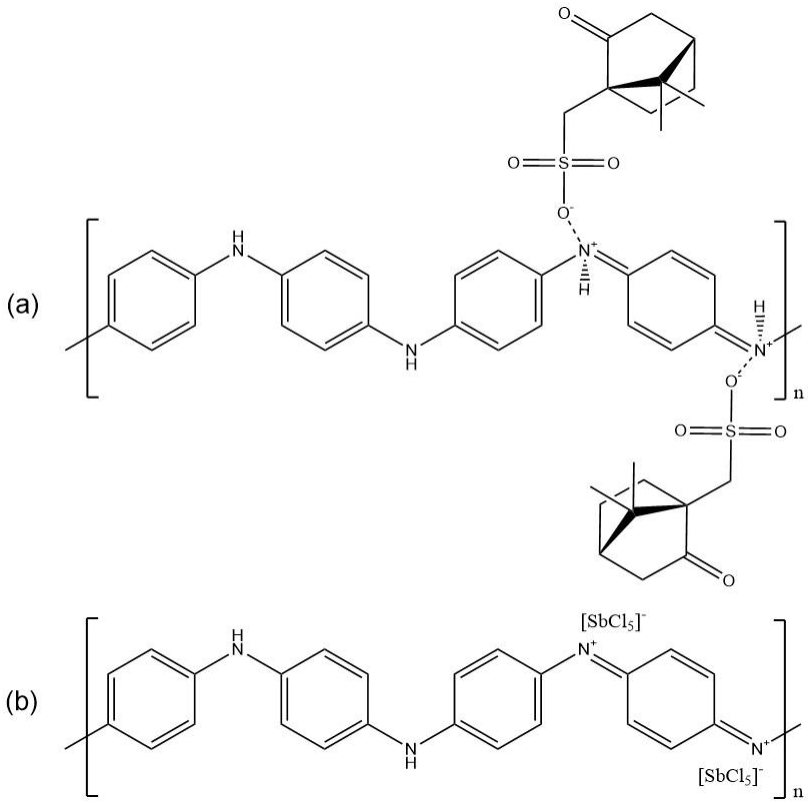

Figure 20. Proposed theoretical fully doped PANI in emeraldine form: (a) CSA-doped and (b) $SbCl_5$-doped polymer.

In the case of PANI produced from CVD, the oxidant $SbCl_5$ acted as a dopant as well, as suggested previously by Smolin *et al.* [41], but unfortunately cannot be detected with this analysis method. Apart from this, CHNS elemental analysis finally gave some insight into the approximate PANI content in these composites, due to a detectable amount of N present in the samples. Assuming that the structure is similar to the one depicted in Figure 20(b), where for the CVD-based sample the N, C, and H contents are 5.82 %, 29.94 %, and 1.87 %, respectively, the total PANI amount in PANI/CNC is only 0.34 wt.% and in PANI/CNF slightly higher – *viz.* 0.43 wt.%, which explains why it was not possible to detect this polymer with previous analysis methods and conductivity could not be measured with the four-point probe.

SEM analysis

Several SEM pictures at different scales were taken for CVD furnished products, which can be seen in Figure 21.

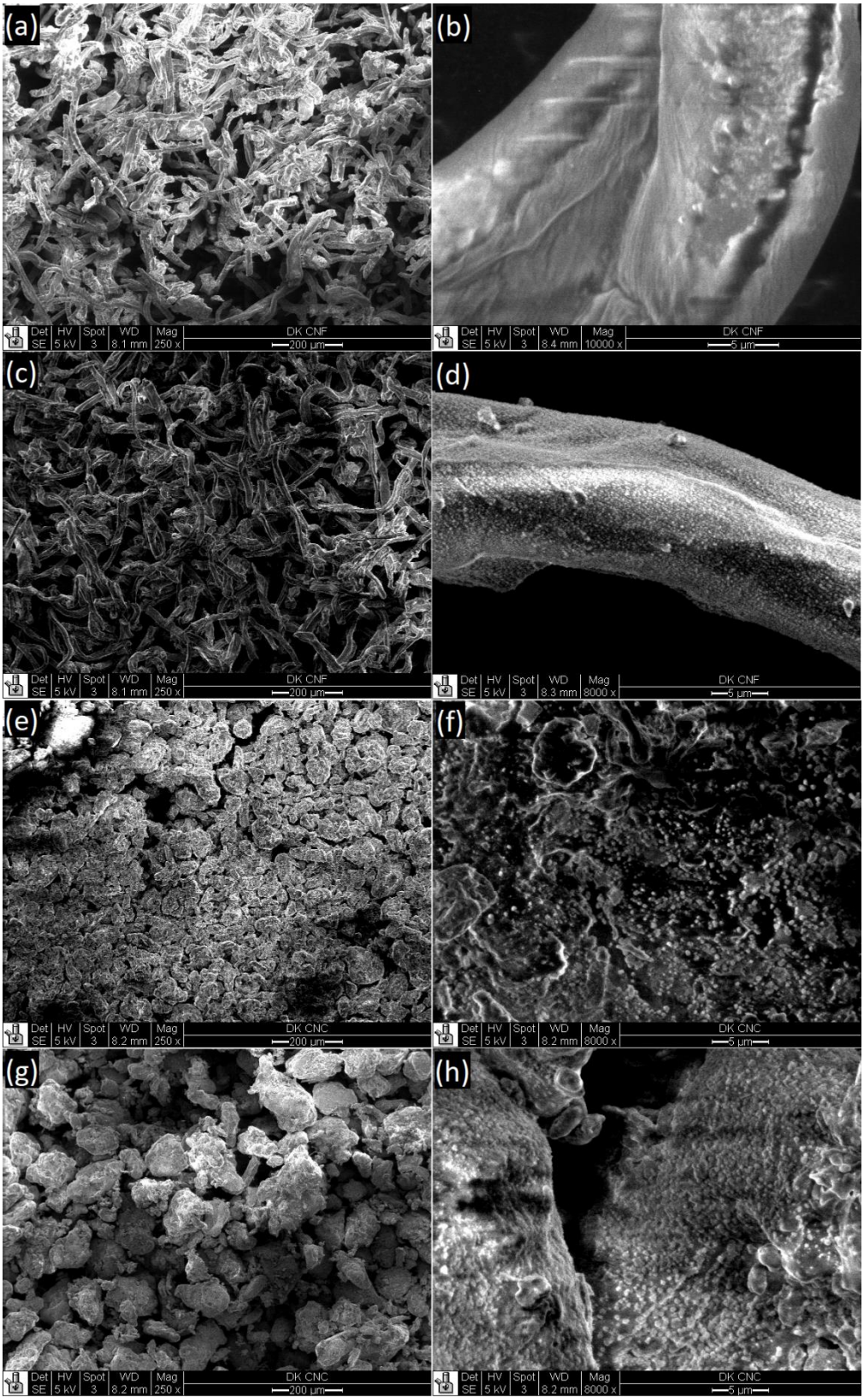

Figure 21. SEM micrographs of untreated CNF at scale (a) 200 µm and (b) 5 µm, CVD furnished PANI/CNF at (c) 200 µm and (d) 5 µm, untreated CNC at (e) 200 µm and (f) 5 µm, CVD furnished PANI/CNC at (g) 200 µm and (h) 5 µm.

Based on these pictures, it was found out that the nanocellulose particles used for the project were significantly larger than expected, untreated and modified CNFs having a diameter of around 10 to 18 µm and CNCs – of around 20 to 50 µm. It is not clear if this is due to a very strong agglomeration of these nanoparticles, even in relatively dry environments, or whether this particle size was already present in the sample received from the manufacturer. Particle agglomeration can be counteracted by using ultrasonication (as was done in the solvent-based approach), while for CVD this is not a feasible option without thoroughly drying the substrate afterwards. Furthermore, the CNC particles had a visibly round shape instead of the expected rod-like shape with a high aspect ratio, which considerably reduces its effectiveness to act as a template for a conductive deposited layer of polymer, when combined with PANI and dispersed in a polymer matrix. Whereas high aspect ratio CNCs, covered with PANI, dispersed in a polymer matrix would give conductive polymer films at relatively low wt.%, for round template particles the percolation threshold would be significantly higher.

When comparing pictures (b) and (d) it is possible to see the distribution of PANI on the fiber, transforming the smooth surface into a seemingly rougher one. A relatively similar micrograph was taken by Müller *et al.* [33] of a composite consisting of bacterial cellulose fibers and HCl-doped PANI. In the case of CNC (pictures (f) and (h)), the difference is not as clearly visible, again due to the extremely low PANI loading.

XPS analysis

XPS is a powerful tool used to not only measure the elemental composition of solids, but also the chemical and electronic state of elements. This analysis technique was applied with the goal to get more insight in the composition of the CVD fabricated products. The low-resolution XPS spectra and high-resolution C 1s spectra of untreated nanocellulose and the composites can be found in Appendix A. For the most part, this data has a close resemblance to spectra of cellulosic samples [70], [71], and the characteristic PANI peaks are not readily visible, due to the very low amount in these composites, as was proven by the CHNS elemental analysis.

Despite this, some trace amounts can be detected. PANI should have a distinctive N 1s peak around 400 eV [72], and therefore a closer look was taken in this range. Figure 22 depicts N 1s spectra of these samples. The untreated nanocellulose had a peak in this range as well, which could elude to some trace amount of impurities in the material. To compare the treated and untreated samples, C/N ratios (C 1s and N 1s peak intensity ratio in the same spectrum) were used as a reliable way to see if there is a detectable increase in N 1s content. And indeed, both the PANI/CNC and PANI/CNF composites exhibited a lowered C/N ratio compared to the pure nanocellulose samples, although in the case of PANI/CNC the difference is quite low. Unfortunately, due to the very low intensity of these peaks, a deeper analysis of the bond structure

for this element was not possible. Nevertheless, the stoichiometric analysis carried out by XPS points out the presence of the polyaniline in the cellulose matrix.

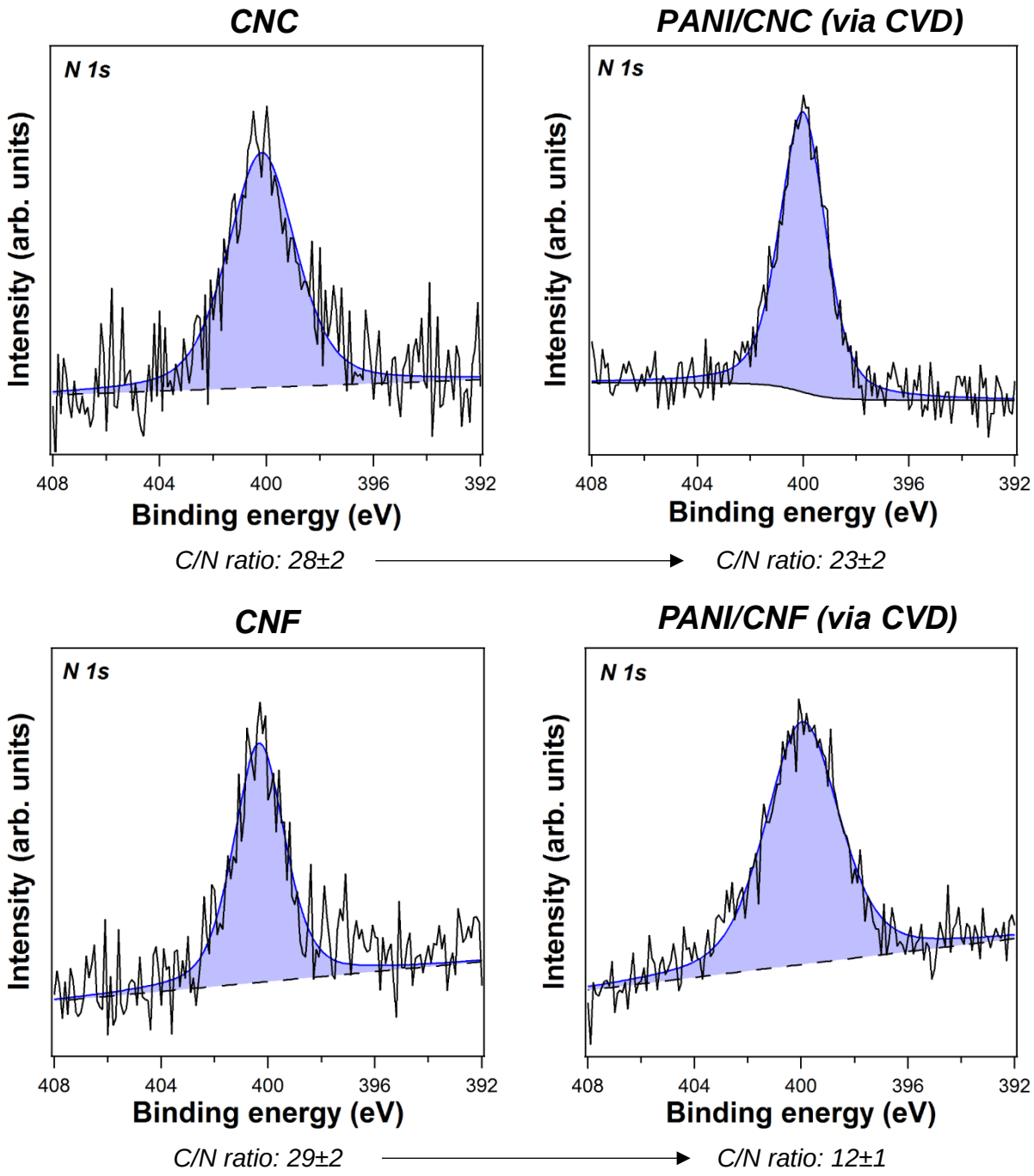

Figure 22. High-resolution N 1s spectra of CNC, CNF, PANI/CNC, PANI/CNF and the corresponding C/N ratios based on the C 1s and N 1s peak intensities of these samples. PANI doping agent: $SbCl_5$.

Figure 23 depicts a better representation of the C/N ratio data of the four samples. This further shows how minimal the C/N ratio is especially between CNC and PANI/CNC if margin of error is taken into account.

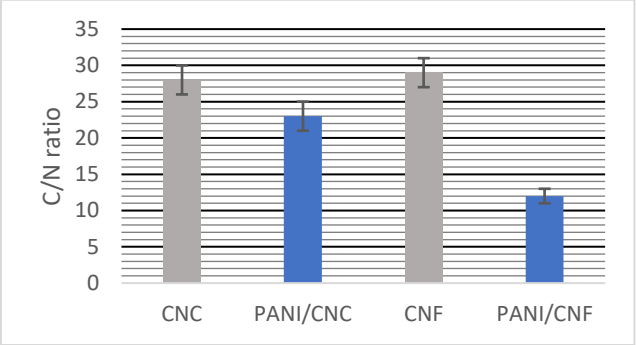

Figure 23. Visualization and comparison of the C/N ratio data between the four XPS samples: CNC, PANI/CNC, CNF, and PANI/CNF. PANI doping agent: $SbCl_5$.

In addition to N, another element that is relevant for these particular materials is Sb, as the oxidant $SbCl_5$ used for CVD acted as the doping agent for the polymer as well and therefore this element directly relates to the doping level of the PANI counterpart in the composites. It was possible to detect slight traces of Sb 4d in the modified samples [73], but not in the pure nanocellulose, as seen in Figure 24, indicating a change in the overall composition. Similarly, no further data can be acquired from these spectra.

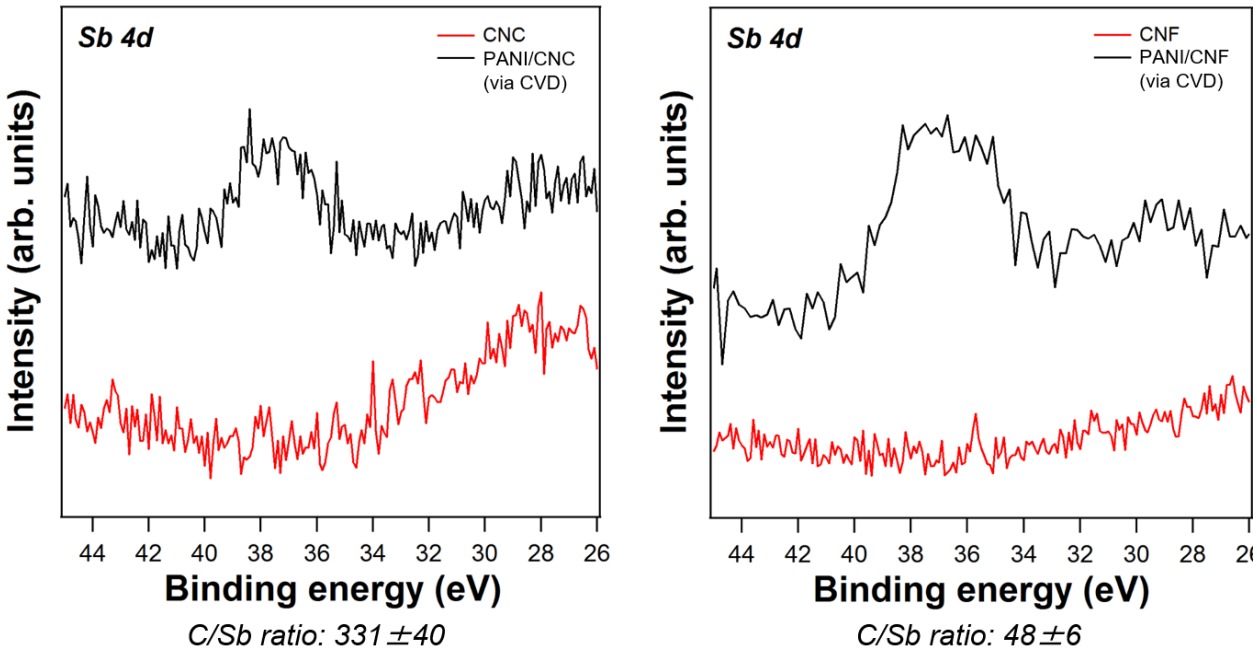

Figure 24. High-resolution spectra in the region of Sb 4d for CNC, CNF, PANI/CNC, PANI/CNF samples and the corresponding C/Sb ratios based on the C 1s and Sb 4d peak intensities of these samples. PANI doping agent: $SbCl_5$

Conductive blends of PANI/CNC with polyurethane

As concluded before, PANI/CNC and PANI/CNF produced from the CVD technique did not have sufficient conductivity to have a further use for the integration in a PU film, and only PANI/CNC composites from the solvent-based method were used to fabricate modified PU films. Products from experiments C5-2 and C6 (Table 4) were applied for this purpose. It was impossible to acquire homogeneous dispersions of these samples in water, if a completely dry material was used due to a strong particle agglomeration. To work around this obstacle, freshly synthesized products with some water content still present were used instead. Water effectively served as a barrier between the composite particles reducing the interactive forces of these structures. Additionally, 2 wt.% SDS was added as a surfactant to improve the dispersion even further. PU coatings with 5 to 50 wt.% PANI/CNC loadings were produced. A measurable conductivity value was acquired for a PU film with approximately 34 wt.% of C5-2 composite – 2.14×10^{-4} S/cm. This sample retained the characteristic dark-green color of PANI and can be seen in Figure 25. A loading of 14 wt.% or lower filler content did not result in a conductive film and therefore the percolation threshold using C5-2 should be between 14 wt.% and 34 wt.%. On the other hand, the C6 product did not yield any samples with high enough electrical conductivity to be measured by the four-point probe, not even at 50 wt.% loading. The high percolation threshold can be explained by the unexpectedly low aspect ratio of the CNC particles as discovered by the SEM analysis.

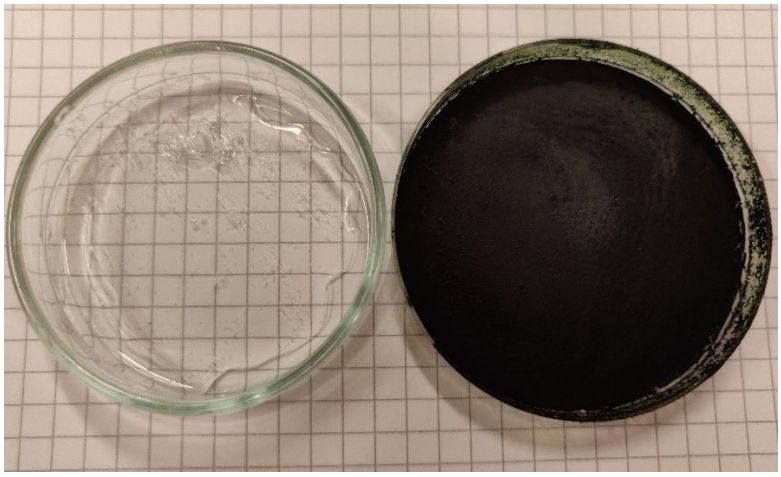

Figure 25. Untreated PU film (left) and modified PU film (right) with 34 wt.% PANI/CNC composite (CNC/aniline = 60/40).

Conclusion

Two very distinct approaches for PANI/CNC composite fabrication were explored in this project. In the solvent-based method it was concluded that the use of an alternative to water, *viz.* the solvent DMSO, did not improve the conductivity of the end product, in spite of the fact that DMSO was expected to enhance the solubility of the polymerizing species and therefore allowing the synthesis of longer polymer chains. CSA-doped PANI showed greater thermal stability compared to the more widely known HCl-doped PANI. The PANI/CNC composites produced via regular chemistry had the underlying issue of strong particle agglomeration which caused difficulties in making good dispersions in water to be mixed with PU. Nonetheless, one successful modified PU film was fabricated using 34 wt.% of PANI/CNC (CNC/Aniline = 60/40) with the conductivity value of 2.14×10^{-4} S/cm. It is assumed that the percolation threshold in this case is below this 34 wt.% mark, but above 14 wt.%, since up to this PANI/CNC filler content no conductivity could be measured. The high percolation threshold could be attributed to the low aspect ratio of the PANI covered particles.

CVD proved to be a much more controlled approach for making thin films, but seemed to be inefficient for small particle modifications, considering that realistically only two coating procedures can be carried out in a day, resulting in only 0.34 – 0.43 wt.% deposition of PANI on 1g of nanocellulose, which was not enough to acquire a composite with a measurable electrical conductivity. The amount of deposited PANI was so low, that it was not possible to detect this polymer with analysis methods other than elemental analysis.

To summarize, a novel conductive material was produced in this project, namely – CSA-doped PANI combined with CNC. This composite was successfully applied as a filler in PU to fabricate a film with potential anti-static properties, due to the conductivity of the material being in the range of 10^{-4} – 10^{-8} S/cm [37]. Furthermore, a proof of concept was established: particle modification with the conductive polymer PANI via the CVD technique is possible, but an insufficient amount of PANI, required for obtaining conductive nanoparticles, is deposited after two sequential CVD treatments.

Further research

As mentioned before, only one successful PANI/CNC modified PU film was produced in this project, due to time constraints. More experiments should be carried out with varying filler content in PU to gain better understanding about the percolation threshold in these particular materials.

Further research should be done in finding alternative dopants for PANI that could lead to better dispersions in water. For example Silva *et al.* [36] concluded that the organic acid DBSA also served as a surfactant, increasing the suspension stability of the produced PANI/CNF particles in an aqueous medium.

When producing PANI/CNC composites, in the pre-synthesis phase where the CNC particles have to be individualized, the use of an ultrasonic probe directly in the solution might be a better alternative to the ultrasonic bath in which the flask was immersed in, since there would be no glass wall anymore, which partially absorbs the applied force need to disperse the particles. A deeper look should be taken into the quality of the individualization of these nanoparticles by the means of cryo-TEM, for example. In addition, more research should possibly be done using CNFs instead of CNCs, as the former tends to have higher aspect ratios.

In the case of CVD, additional coating cycles should be carried out to see at what PANI content the composite would exhibit measurable conductivity. Furthermore, it could be possible to further optimize the experimental procedure by adjusting the flow rates, deposition duration, substrate temperature etc. Added post-treatment of the product might improve the desired properties, such as washing with solvents or de-doping and re-doping with a different acid. Smolin et al. [41] discovered that washing with THF improved the quality of the deposited PANI film. Finally, it would be interesting to investigate the feasibility of a rotating particle bed oCVD reactor to coat small particles such as nanocellulose. A similar concept had already been realized before with positive results, but only for iCVD [55], [56].

References

[1] X. Du, Z. Zhang, W. Liu, and Y. Deng, "Nanocellulose-based conductive materials and their emerging applications in energy devices - A review," *Nano Energy*, vol. 35, no. May 2018, pp. 299–320, May 2017.

[2] W. E. Tenhaeff and K. K. Gleason, "Initiated and Oxidative Chemical Vapor Deposition of Polymeric Thin Films: iCVD and oCVD," *Adv. Funct. Mater.*, vol. 18, no. 7, pp. 979–992, Apr. 2008.

[3] S. Bhadra, D. Khastgir, N. K. Singha, and J. H. Lee, "Progress in preparation, processing and applications of polyaniline," *Prog. Polym. Sci.*, vol. 34, no. 8, pp. 783–810, 2009.

[4] "Chemical Vapor Deposition Explained. Its Benefits and Drawbacks." [Online]. Available: https://www.silcotek.com/semi-coating-blog/chemical-vapor-deposition-explained.-its-benefits-and-drawbacks. [Accessed: 03-Jun-2019].

[5] X. Li *et al.*, "Polyaniline on surface modification of diatomite: A novel way to obtain conducting diatomite fillers," *Appl. Surf. Sci.*, vol. 207, no. 1–4, pp. 378–383, 2003.

[6] H. Yu, P. Chen, W. Chen, and Y. Liu, "Effect of cellulose nanofibers on induced polymerization of aniline and formation of nanostructured conducting composite," *Cellulose*, vol. 21, no. 3, pp. 1757–1767, Jun. 2014.

[7] M. Nasir, R. Hashim, O. Sulaiman, and M. Asim, "Nanocellulose: Preparation methods and applications," in *Cellulose-Reinforced Nanofibre Composites: Production, Properties and Applications*, Elsevier Ltd, 2017, pp. 261–276.

[8] P. Lu and Y.-L. Hsieh, "Preparation and characterization of cellulose nanocrystals from rice straw," *Carbohydr. Polym.*, vol. 87, no. 1, pp. 564–573, Jan. 2012.

[9] J. Unsworth, B. A. Lunn, P. C. Innis, Z. Jin, A. Kaynak, and N. G. Booth, "Technical Review: Conducting Polymer Electronics," *J. Intell. Mater. Syst. Struct.*, vol. 3, no. 3, pp. 380–395, 1992.

[10] S. Bhadra, N. K. Singha, and D. Khastgir, "Polyaniline by new miniemulsion polymerization and the effect of reducing agent on conductivity," *Synth. Met.*, vol. 156, no. 16–17, pp. 1148–1154, 2006.

[11] E. M. Geniès, A. Boyle, M. Lapkowski, and C. Tsintavis, "Polyaniline: A historical survey," *Synth. Met.*, vol. 36, no. 2, pp. 139–182, 1990.

[12] K. M. Dinesan and A. A. Syed, "Review: Polyaniline - A Novel Polymeric Material," *Talanta*, vol. 38, no. 8, pp. 815–837, 1991.

[13] D. Li, J. Huang, and R. B. Kaner, "Polyaniline Nanofibers: A Unique Polymer Nanostructure for Versatile Applications," *Acc. Chem. Res.*, vol. 40, no. 16, pp. 135–145, Apr. 2009.

[14] Z. A. Boeva and V. G. Sergeyev, "Polyaniline : Synthesis , Properties , and Application," *Polym. Sci. Ser. C*, vol. 56, no. 1, pp. 144–153, 2014.

[15] D. Nicolas-Debarnot and F. Poncin-Epaillard, “Polyaniline as a new sensitive layer for gas sensors,” *Anal. Chim. Acta*, vol. 475, no. 1–2, pp. 1–15, 2003.

[16] K. Lee, S. Cho, H. P. Sung, A. J. Heeger, C. W. Lee, and S. H. Lee, “Metallic transport in polyaniline,” *Nature*, vol. 441, no. 1, pp. 65–68, 2006.

[17] R. G. Bavane, “Synthesis and characterization of thin films of conducting polymers for gas sensing applications. Chapter 3: Synthesis of Polyaniline (PANI),” North Maharashtra University, 2014.

[18] A. Mostafaei and A. Zolriasatein, “Synthesis and characterization of conducting polyaniline nanocomposites containing ZnO nanorods,” *Prog. Nat. Sci. Mater. Int.*, vol. 22, no. 4, pp. 273–280, 2012.

[19] R. L. Razalli, M. M. Abdi, P. M. Tahir, A. Moradbak, Y. Sulaiman, and L. Y. Heng, “Polyaniline-modified nanocellulose prepared from Semantan bamboo by chemical polymerization: preparation and characterization,” *RSC Adv.*, vol. 7, no. 41, pp. 25191–25198, 2017.

[20] I. Gawri, S. Khatta, K. P. Singh, and S. K. Tripathi, “Synthesis and Characterization of Polyaniline as Emeraldine Salt,” *Am. Inst. Phys.*, vol. 1728, no. 1, pp. 1–4, 2016.

[21] S. B. Abel, E. I. Yslas, C. R. Rivarola, and C. A. Barbero, “Synthesis of polyaniline (PANI) and functionalized polyaniline (F-PANI) nanoparticles with controlled size by solvent displacement method. Application in fluorescence detection and bacteria killing by photothermal effect,” *Nanotechnology*, vol. 29, no. 12, p. 125604, Mar. 2018.

[22] V. P. Anju and S. K. Narayanankutty, “Polyaniline coated cellulose fiber / polyvinyl alcohol composites with high dielectric permittivity and low percolation threshold,” *AIP Adv.*, vol. 6, no. 1, p. 015109, Jan. 2016.

[23] F. G. Souza, G. E. Oliveira, C. H. M. Rodrigues, B. G. Soares, M. Nele, and J. C. Pinto, “Natural Brazilian Amazonic (Curauá) Fibers Modified with Polyaniline Nanoparticles,” *Macromol. Mater. Eng.*, vol. 294, no. 8, pp. 484–491, Aug. 2009.

[24] B. I. Hassel, S. M. Trey, S. Leijonmarck, and M. Johansson, “A Study on the Morphology, Mechanical, and Electrical Performance of Polyaniline-modified Wood - A Semiconducting Composite Material,” *BioResources*, vol. 9, no. 3, pp. 5007–5023, 2014.

[25] G. Ciric-Marjanovic, “Recent advances in polyaniline research: Polymerization mechanisms, structural aspects, properties and applications,” *Synth. Met.*, vol. 177, no. 3, pp. 1–47, 2013.

[26] S. I. A. Razak *et al.*, “Coating of Conducting Polymers on Natural Cellulosic Fibers,” in *Conducting Polymers*, no. December, InTech, 2016.

[27] M. Teli, S. Dash, and P. Desai, “Polyaniline Based Conductive Textiles,” *J. Inst. Eng. Ser. E*, vol. 95, no. 2, pp. 75–79, Dec. 2014.

[28] W. He, X. Zhang, C. Yu, D. Huang, and Y. Li, “Synthesis of Bamboo/Polyaniline Composites by

In Situ Polymerization and Their Characteristics," *BioResources*, vol. 10, no. 2, pp. 2969–2981, 2015.

[29] F. G. Souza, A. M. da Silva, G. E. de Oliveira, R. M. Costa, E. R. Fernandes, and E. D. Pereira, "Conducting and magnetic mango fibers," *Ind. Crops Prod.*, vol. 68, no. June 2018, pp. 97–104, Jun. 2015.

[30] S. I. A. Razak, W. A. W. A. Rahman, S. Hashim, and M. Y. Yahya, "In situ surface modification of natural fiber by conducting polyaniline," *Compos. Interfaces*, vol. 19, no. 6, pp. 365–376, Aug. 2012.

[31] V. Bajgar *et al.*, "Cotton Fabric Coated with Conducting Polymers and its Application in Monitoring of Carnivorous Plant Response," *Sensors*, vol. 16, no. 4, p. 498, Apr. 2016.

[32] J. A. Marins, B. G. Soares, K. Dahmouche, S. J. L. Ribeiro, H. Barud, and D. Bonemer, "Structure and properties of conducting bacterial cellulose-polyaniline nanocomposites," *Cellulose*, vol. 18, no. 5, pp. 1285–1294, 2011.

[33] D. Müller *et al.*, "Electrically conducting nanocomposites: Preparation and properties of polyaniline (PAni)-coated bacterial cellulose nanofibers (BC)," *Cellulose*, vol. 19, no. 5, pp. 1645–1654, 2012.

[34] B. H. Lee, H. J. Kim, and H. S. Yang, "Polymerization of aniline on bacterial cellulose and characterization of bacterial cellulose/polyaniline nanocomposite films," *Curr. Appl. Phys.*, vol. 12, no. 1, pp. 75–80, 2012.

[35] U. M. Casado, M. I. Aranguren, and N. E. Marcovich, "Preparation and characterization of conductive nanostructured particles based on polyaniline and cellulose nanofibers," *Ultrason. Sonochem.*, vol. 21, no. 5, pp. 1641–1648, Sep. 2014.

[36] M. J. Silva *et al.*, "Conductive Nanocomposites Based on Cellulose Nanofibrils Coated with Polyaniline-DBSA Via In Situ Polymerization," *Macromol. Symp.*, vol. 319, no. 1, pp. 196–202, Sep. 2012.

[37] G. A. Gelves, M. H. Al-Saleh, and U. Sundararaj, "Highly electrically conductive and high performance EMI shielding nanowire/polymer nanocomposites by miscible mixing and precipitation," *J. Mater. Chem.*, vol. 21, no. 3, pp. 829–836, 2011.

[38] C. Merlini *et al.*, "Polyaniline-coated coconut fibers: Structure, properties and their use as conductive additives in matrix of polyurethane derived from castor oil," *Polym. Test.*, vol. 38, pp. 18–25, Sep. 2014.

[39] M. L. Auad *et al.*, "Polyaniline-modified cellulose nanofibrils as reinforcement of a smart polyurethane," *Polym. Int.*, vol. 60, no. 5, pp. 743–750, May 2011.

[40] K. K. Gleason, *CVD Polymers: Fabrication of Organic Surfaces and Devices*. Weinheim, Germany: Wiley-VCH Verlag GmbH & Co. KGaA, 2015.

[41] Y. Y. Smolin, M. Soroush, and K. K. S. Lau, "Oxidative chemical vapor deposition of polyaniline thin films," *Beilstein J. Nanotechnol.*, vol. 8, no. 1, pp. 1266–1276, Jun. 2017.

[42] X. Li, A. Rafie, Y. Y. Smolin, S. Simotwo, V. Kalra, and K. K. S. Lau, "Engineering conformal nanoporous polyaniline via oxidative chemical vapor deposition and its potential application in supercapacitors," *Chem. Eng. Sci.*, vol. 194, pp. 156–164, Feb. 2019.

[43] Y. Y. Smolin, K. L. Van Aken, M. Boota, M. Soroush, Y. Gogotsi, and K. K. S. Lau, "Engineering Ultrathin Polyaniline in Micro/Mesoporous Carbon Supercapacitor Electrodes Using Oxidative Chemical Vapor Deposition," *Adv. Mater. Interfaces*, vol. 4, no. 8, p. 1601201, Apr. 2017.

[44] Y. Y. Smolin, M. Soroush, and K. K. S. Lau, "Influence of oCVD Polyaniline Film Chemistry in Carbon-Based Supercapacitors," *Ind. Eng. Chem. Res.*, vol. 56, no. 21, pp. 6221–6228, 2017.

[45] B. Reeja-Jayan *et al.*, "A Route Towards Sustainability Through Engineered Polymeric Interfaces," *Adv. Mater. Interfaces*, vol. 1, no. 4, p. 1400117, Jul. 2014.

[46] S. Nejati and K. K. S. Lau, "Chemical Vapor Deposition Synthesis of Tunable Unsubstituted Polythiophene," *Langmuir*, vol. 27, no. 24, pp. 15223–15229, Dec. 2011.

[47] H. Chelawat, S. Vaddiraju, and K. Gleason, "Conformal, Conducting Poly(3,4-ethylenedioxythiophene) Thin Films Deposited Using Bromine as the Oxidant in a Completely Dry Oxidative Chemical Vapor Deposition Process," *Chem. Mater.*, vol. 22, no. 9, pp. 2864–2868, May 2010.

[48] N. Lachman *et al.*, "Tailoring Thickness of Conformal Conducting Polymer Decorated Aligned Carbon Nanotube Electrodes for Energy Storage," *Adv. Mater. Interfaces*, vol. 1, no. 7, p. 1400076, Oct. 2014.

[49] Y. Zhou *et al.*, "A high performance hybrid asymmetric supercapacitor via nano-scale morphology control of graphene, conducting polymer, and carbon nanotube electrodes," *J. Mater. Chem. A*, vol. 2, no. 26, pp. 9964–9969, 2014.

[50] D. Bhattacharyya, R. Yang, and K. K. Gleason, "High aspect ratio, functionalizable conducting copolymer nanobundles," *J. Mater. Chem.*, vol. 22, no. 33, p. 17147, 2012.

[51] S. Vaddiraju, H. Cebeci, K. K. Gleason, and B. L. Wardle, "Hierarchical Multifunctional Composites by Conformally Coating Aligned Carbon Nanotube Arrays with Conducting Polymer," *ACS Appl. Mater. Interfaces*, vol. 1, no. 11, pp. 2565–2572, Nov. 2009.

[52] Y. Ye, Y. Mao, H. Wang, and Z. Ren, "Hybrid structure of pH-responsive hydrogel and carbon nanotube array with superwettability," *J. Mater. Chem.*, vol. 22, no. 6, pp. 2449–2455, 2012.

[53] R. K. Bose, A. M. Heming, and K. K. S. Lau, "Microencapsulation of a Crop Protection Compound by Initiated Chemical Vapor Deposition," *Macromol. Rapid Commun.*, vol. 33, no. 16, pp. 1375–1380, Aug. 2012.

[54] S. H. Baxamusa, L. Montero, J. M. Dubach, H. A. Clark, S. Borros, and K. K. Gleason, “Protection of Sensors for Biological Applications by Photoinitiated Chemical Vapor Deposition of Hydrogel Thin Films,” *Biomacromolecules*, vol. 9, no. 10, pp. 2857–2862, Oct. 2008.

[55] K. K. S. Lau and K. K. Gleason, “Particle Surface Design using an All-Dry Encapsulation Method,” *Adv. Mater.*, vol. 18, no. 15, pp. 1972–1977, Aug. 2006.

[56] T. C. Parker, D. Baechle, and J. D. Demaree, “Polymeric barrier coatings via initiated chemical vapor deposition,” *Surf. Coatings Technol.*, vol. 206, no. 7, pp. 1680–1683, Dec. 2011.

[57] M. N. Subramaniam, P. S. Goh, W. J. Lau, A. F. Ismail, M. Gürsoy, and M. Karaman, “Synthesis of Titania nanotubes/polyaniline via rotating bed-plasma enhanced chemical vapor deposition for enhanced visible light photodegradation,” *Appl. Surf. Sci.*, vol. 484, no. December 2018, pp. 740–750, Aug. 2019.

[58] “Crystalline Nanocellulose (Nanocrystalline Cellulose).” [Online]. Available: https://nanografi.com/nanoparticles/cellulose-nanocrystal-nanocrystalline-cellulose-cnc/. [Accessed: 26-Jun-2019].

[59] “Nanofibrillated Cellulose (Cellulose Nanofibril).” [Online]. Available: https://nanografi.com/nanoparticles/cellulose-nanofiber-cellulose-nanofibril-nanofibrillated-cellulose-cnfs/. [Accessed: 26-Jun-2019].

[60] A. G. MacDiarmid and A. J. Epstein, “The concept of secondary doping as applied to polyaniline,” *Synth. Met.*, vol. 65, no. 2–3, pp. 103–116, Aug. 1994.

[61] Y. Cao, P. Smith, and A. J. Heeger, “Counter-ion induced processibility of conducting polyaniline and of conducting polyblends of polyaniline in bulk polymers,” *Synth. Met.*, vol. 48, no. 1, pp. 91–97, Jun. 1992.

[62] M. G. Han, Y. J. Lee, S. W. Byun, and S. S. Im, “Physical properties and thermal transition of polyaniline film,” *Synth. Met.*, vol. 124, no. 2–3, pp. 337–343, Oct. 2001.

[63] C. Kim, W. Oh, and J. W. Park, “Solid/liquid interfacial synthesis of high conductivity polyaniline,” *RSC Adv.*, vol. 6, no. 86, pp. 82721–82725, 2016.

[64] K. Newell, “The Effects of Water on DMSO and Effective Hydration Measurement.” [Online]. Available: http://www.ziath.com/images/pdf/DMSO_The_effects_of_water_and_hydration_measurement.pdf. [Accessed: 29-Jun-2019].

[65] M. Trchová and J. Stejskal, “Polyaniline: The infrared spectroscopy of conducting polymer nanotubes (IUPAC Technical Report),” *Pure Appl. Chem.*, vol. 83, no. 10, pp. 1803–1817, Jun. 2011.

[66] J. Kumar *et al.*, “Highly Sensitive Chemo-Resistive Ammonia Sensor Based on Dodecyl Benzene

Sulfonic Acid Doped Polyaniline Thin Film," *Sci. Adv. Mater.*, vol. 7, no. 3, pp. 518–525, 2015.

[67] R. S. Biscaro, R. Faez, and M. C. Rezende, "Reactive doping of PAni-CSA and its use in microwave absorbing materials," *Polym. Adv. Technol.*, vol. 20, no. 1, pp. 28–34, Jan. 2009.

[68] Q. Wu, Y.-F. Qin, L. Chen, and Z.-Y. Qin, "Conductive Polyaniline/Cellulose Nanocrystals Composite for Ammonia Gas Detection," in *Computer Science and Engineering Technology (CSET2015), Medical Science and Biological Engineering (MSBE2015)*, 2016, no. January, pp. 670–675.

[69] C. Dhand *et al.*, "Preparation, characterization and application of polyaniline nanospheres to biosensing," *Nanoscale*, vol. 2, no. 5, p. 747, 2010.

[70] L.-S. Johansson and J. M. Campbell, "Reproducible XPS on biopolymers: cellulose studies," *Surf. Interface Anal.*, vol. 36, no. 8, pp. 1018–1022, Aug. 2004.

[71] C. Huang, Q. Yang, and S. Wang, "XPS characterization of fiber surface of chemithermomechanical pulp fibers modified by white-rot fungi," *Asian J. Chem.*, vol. 24, no. 12, pp. 5476–5480, 2012.

[72] S. H. Patil, A. P. Gaikwad, S. D. Sathaye, and K. R. Patil, "To form layer by layer composite film in view of its application as supercapacitor electrode by exploiting the techniques of thin films formation just around the corner," *Electrochim. Acta*, vol. 265, pp. 556–568, Mar. 2018.

[73] "NIST XPS Database Detail Page." [Online]. Available: https://srdata.nist.gov/xps/XPSDetailPage.aspx?AllDataNo=30391. [Accessed: 01-Aug-2019].

Appendix: XPS additional data

Appendix 1: XPS low-resolution scan spectra

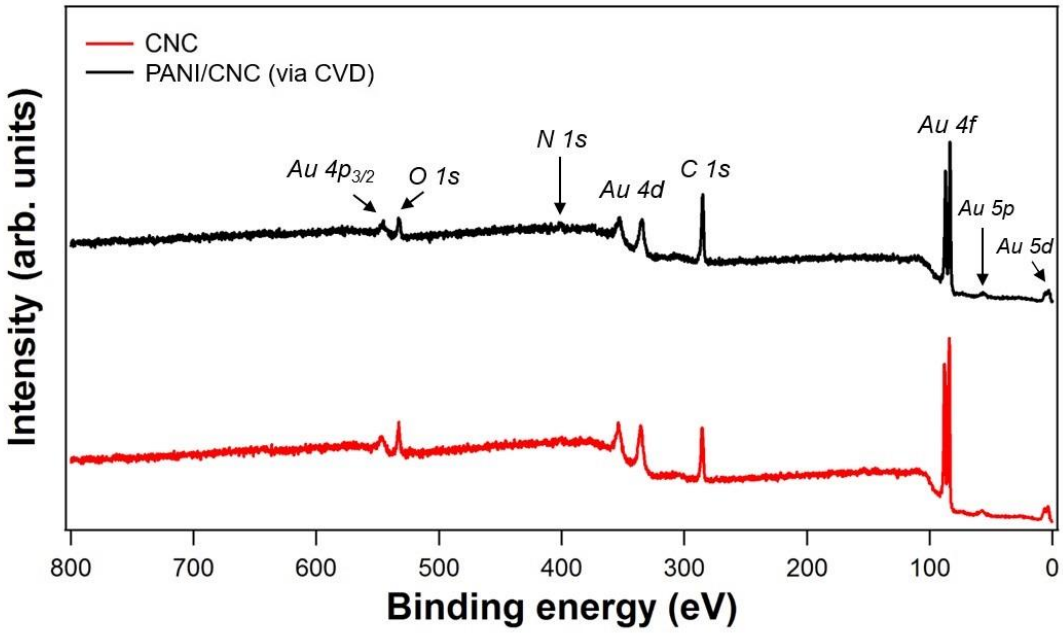

Figure 26. Low-resolution spectra of CNC and PANI/CNC, highlighting the relevant XPS peaks. Note: peaks of Au are related to the substrate holder. PANI doping agent: $SbCl_5$.

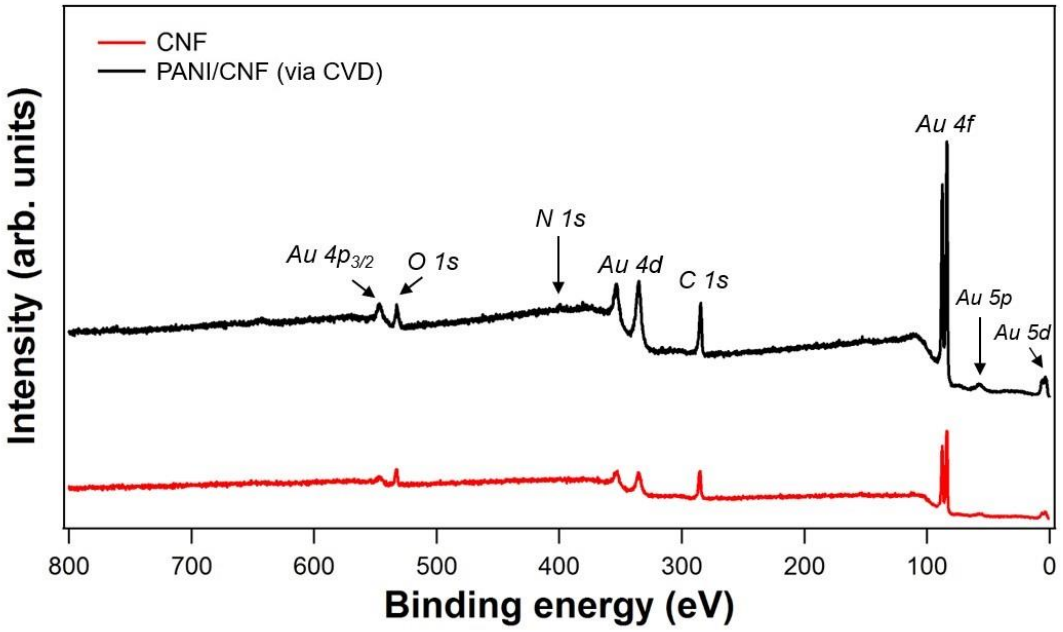

Figure 27. Low-resolution spectra of CNF and PANI/CNF, highlighting the relevant XPS peaks. Note: peaks of Au are related to the substrate holder. PANI doping agent: $SbCl_5$.

Appendix 2: XPS C 1s spectra

Note: due to uncertainties in the fitting of the spectra, all percentages of separate components have an error bar of about 2%.

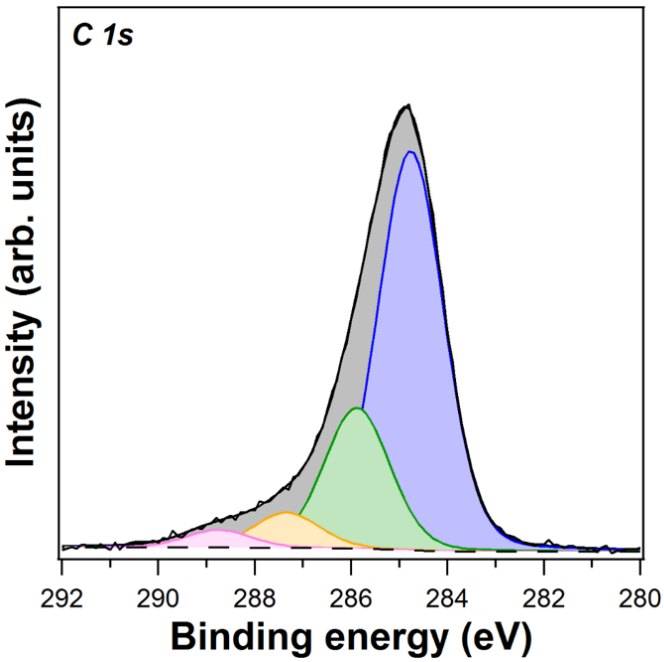

Species	B.E. (eV)	Width (eV)	% Area
C-C/C=C	284.8	1.6	67.2
C-O/C-N	285.9	1.6	23.8
O-C-O/ C=O	287.4	1.6	6.0
O=C-O	288.8	1.6	3.0

Figure 28. High-resolution C 1s spectrum of CNC with the decomposition map of the relevant species.

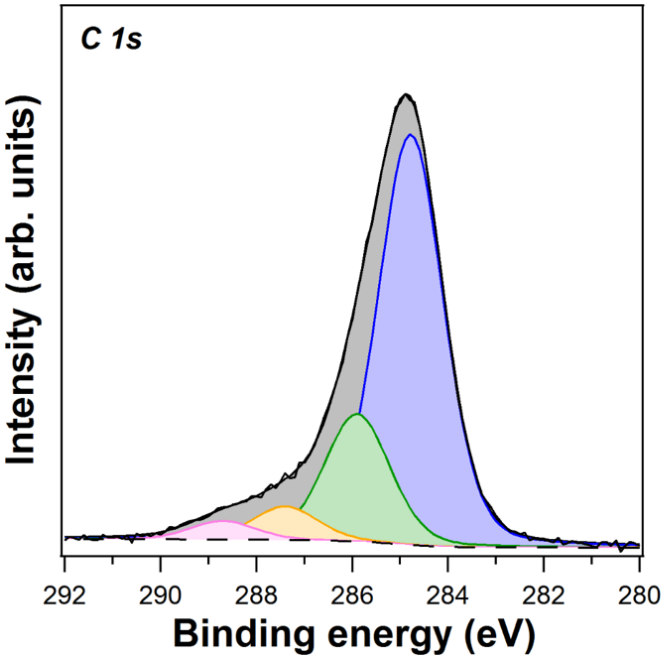

Species	B.E. (eV)	Width (eV)	% Area
C-C/C=C	284.8	1.6	69.5
C-O/C-N	285.9	1.6	21.6
O-C-O/ C=O	287.4	1.6	5.7
O=C-O	288.7	1.6	3.2

Figure 29. High-resolution C 1s spectrum of PANI/CNC (produced from CVD) with the decomposition map of the relevant species. PANI doping agent: $SbCl_5$.

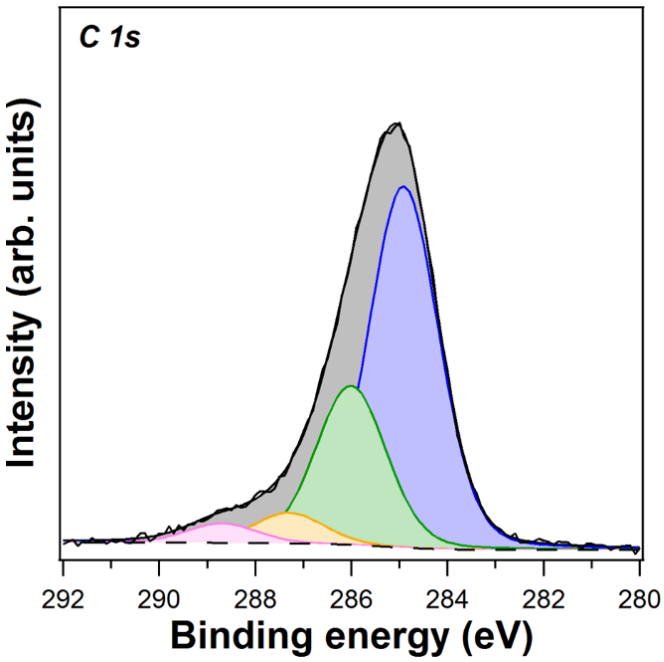

Species	B.E. (eV)	Width (eV)	% Area
C-C/C=C	284.8	1.7	63.3
C-O/C-N	285.9	1.7	27.9
O-C-O/ C=O	287.2	1.7	5.4
O=C-O	288.5	1.7	3.4

Figure 30. High-resolution C 1s spectrum of CNF with the decomposition map of the relevant species.

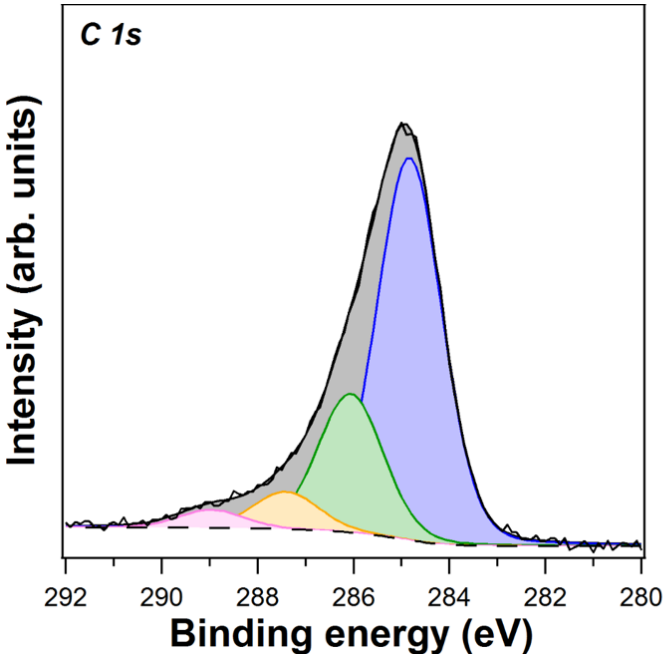

Species	B.E. (eV)	Width (eV)	% Area
C-C/C=C	284.8	1.6	66.3
C-O/C-N	286.1	1.6	24.0
O-C-O/ C=O	287.4	1.6	6.5
O=C-O	289.0	1.6	3.2

Figure 31. High-resolution C 1s spectrum of PANI/CNF (produced from CVD) with the decomposition map of the relevant species. PANI doping agent: $SbCl_5$.